



Extensive Thioautotrophic Gill Endosymbiont Diversity within a Single *Ctena orbiculata* (Bivalvia: Lucinidae) Population and Implications for Defining Host-Symbiont Specificity and Species Recognition

Shen Jean Lim,^a Louie Alexander,^a  Annette Summers Engel,^b Audrey T. Paterson,^b Laurie C. Anderson,^c Barbara J. Campbell^a

^aDepartment of Biological Sciences, Clemson University, Clemson, South Carolina, USA

^bDepartment of Earth and Planetary Sciences, University of Tennessee—Knoxville, Knoxville, Tennessee, USA

^cDepartment of Geology and Geological Engineering, South Dakota School of Mines & Technology, Rapid City, South Dakota, USA

ABSTRACT Seagrass-dwelling members of the bivalve family Lucinidae harbor environmentally acquired gill endosymbionts. According to previous studies, lucinid symbionts potentially represent multiple strains from a single thioautotrophic gamma-proteobacterium species. This study utilized genomic- and transcriptomic-level data to resolve symbiont taxonomic, genetic, and functional diversity from *Ctena orbiculata* endosymbiont populations inhabiting carbonate-rich sediment at Sugarloaf Key, FL (USA). The sediment had mixed seagrass and calcareous green alga coverage and also was colonized by at least five other lucinid species. Four coexisting, thioautotrophic endosymbiont operational taxonomic units (OTUs), likely representing four strains from two different bacterial species, were identified from *C. orbiculata*. Three of these OTUs also occurred at high relative abundances in the other sympatric lucinid species. Interspecies genetic differences averaged about 5% lower at both pairwise average nucleotide identity and amino acid identity than interstrain differences. Despite these genetic differences, *C. orbiculata* endosymbionts shared a high number of metabolic functions, including highly expressed thioautotrophy-related genes and a moderately to weakly expressed conserved one-carbon (C₁) oxidation gene cluster previously undescribed in lucinid symbionts. Few symbiont- and host-related genes, including those encoding symbiotic sulfurtransferase, host respiratory functions, and host sulfide oxidation functions, were differentially expressed between seagrass- and alga-covered sediment locations. In contrast to previous studies, the identification of multiple endosymbiont taxa within and across *C. orbiculata* individuals, which were also shared with other sympatric lucinid species, suggests that neither host nor endosymbiont displays strict taxonomic specificity. This necessitates further investigations into the nature and extent of specificity of lucinid hosts and their symbionts.

IMPORTANCE Symbiont diversity and host/symbiont functions have been comprehensively profiled for only a few lucinid species. In this work, unprecedented thioautotrophic gill endosymbiont taxonomic diversity was characterized within a *Ctena orbiculata* population associated with both seagrass- and alga-covered sediments. Endosymbiont metabolisms included known chemosynthetic functions and an additional conserved, previously uncharacterized C₁ oxidation pathway. Lucinid-symbiont associations were not species specific because this *C. orbiculata* population hosted multiple endosymbiont strains and species, and other sympatric lucinid species shared overlapping symbiont 16S rRNA gene diversity profiles with *C. orbiculata*. Our results suggest that lucinid-symbiont association patterns within some host species could be more taxonomically diverse than previously thought. As such, this study

Citation Lim SJ, Alexander L, Engel AS, Paterson AT, Anderson LC, Campbell BJ. 2019. Extensive thioautotrophic gill endosymbiont diversity within a single *Ctena orbiculata* (Bivalvia: Lucinidae) population and implications for defining host-symbiont specificity and species recognition. mSystems 4:e00280-19. <https://doi.org/10.1128/mSystems.00280-19>.

Editor Holly Bik, University of California, Riverside

Copyright © 2019 Lim et al. This is an open-access article distributed under the terms of the [Creative Commons Attribution 4.0 International license](https://creativecommons.org/licenses/by/4.0/).

Address correspondence to Barbara J. Campbell, bcampb7@clemson.edu.

 Species- and strain-level thioautotrophic gill endosymbiont diversity in the lucinid bivalve *Ctena orbiculata* associated with seagrass and algae sediments

Received 1 May 2019

Accepted 6 August 2019

Published 27 August 2019

highlights the importance of holistic analyses, at the population, community, and even ecosystem levels, in understanding host-microbe association patterns.

KEYWORDS host-microbe interactions, lucinid, metagenomics, metatranscriptomics, symbiosis

Chemolithoautotrophic symbiosis, where symbiotic bacteria use inorganic chemical energy for the synthesis of organic compounds that benefit their hosts, is prevalent in marine bivalves, including the Lucinidae (1, 2). All extant lucinid species examined to date host chemosynthetic bacterial endosymbionts belonging to the class *Gammaproteobacteria* within specialized epithelial gill cells known as bacteriocytes (3). Lucinid gill endosymbionts possess a diverse and varied suite of functions, including thioautotrophy (4), aerobic respiration (5), assimilatory and dissimilatory nitrate reduction (6), mixotrophy (7, 8), hydrogenotrophy (7, 8), and diazotrophy (7, 9), which enable lucinids to colonize otherwise uninhabitable conditions (10). Specifically, lucinids burrow into sediments where oxygen is available from the oxic water column and dissolved sulfide is present due to the decomposition of organic matter via sulfate reduction (2, 3, 11). In modern seagrass habitats, a three-way symbiotic association among bacteria, lucinids, and seagrass has been proposed (11, 12). Lucinid hosts acquire oxygen for respiration from oxygenated water surrounding seagrass roots, and the thioautotrophic endosymbionts oxidize sulfide while fixing inorganic carbon for the host (12). Seagrass growth is promoted because the endosymbionts remove sulfide and have the potential to fix nitrogen (7, 11, 12). This symbiotic system likely developed in the late Cretaceous period, based on the correspondence of adaptive radiation of shallow marine lucinid species in the fossil record to the evolutionary first appearances of marine angiosperms, including seagrasses (13).

Lucinid gill endosymbionts are related to a larger group of diverse marine thioautotrophic symbionts (1). However, unlike chemosymbiotic Solemyidae and Vesicomysiidae bivalves, where vertical or mixed symbiont transmission has been observed (14–16), lucinids studied to date acquire their endosymbionts environmentally (17–19). Based on their 16S rRNA gene sequences, lucinid endosymbionts occur in three distinct clades, with the largest (clade A) originating from hosts that primarily inhabit sediments from seagrass beds and two (clades B and C) originating from lucinids that are more likely to inhabit sediments from mangrove-rich areas (20). It is possible that each clade represents a separate species (8), although an insufficient number of lucinid species has been examined at a sufficiently high genetic resolution to test this hypothesis. At present, low to no variability among clade A lucinid endosymbiont 16S rRNA gene sequences suggests that this group belongs to a single species (20–23). Earlier studies of gill thioautotrophic endosymbionts from lesser Antillean lucinid hosts, including *Ctena imbricatula* (referred to as *Codakia orbiculata* in reference 21), *Codakia orbicularis*, *Parvilucina pectinella* (referred to as *Codakia pectinella* in reference 21), *Anodontia alba*, *Divalinga quadrisulcata* (referred to as *Divaricella quadrisulcata* in reference 21), and *Lucina roquesana* (referred to as *Linga pensylvanica* in reference 21), show identical 16S rRNA gene sequences (22, 23) and the capability of infecting aposymbiotic *Codakia orbicularis* juveniles (24). Recent reanalysis of these thioautotrophic endosymbionts using five other marker genes (instead of the slow-evolving 16S rRNA gene) revealed that intraspecific symbiont strain diversity in the population was shaped by host geographic location (25). Strain-specific symbiont acquisition was also observed in the same study (25), where starved *Ctena imbricatula* individuals (referred to as *Codakia orbiculata* in reference 21) could reacquire only the exact symbiont strain that they initially hosted before starvation. This suggests that, unlike undifferentiated naive bacteriocytes, mature bacteriocytes can possibly recognize and select specific chemolithoautotrophic symbiont strains (24, 25).

In spite of these findings, species- and strain-level diversity within lucinid endosymbiont clades remains unverified for most lucinid species. To date, endosymbiont functions for two clade A endosymbionts, "*Candidatus* Thiodiazotropha endolucinida"

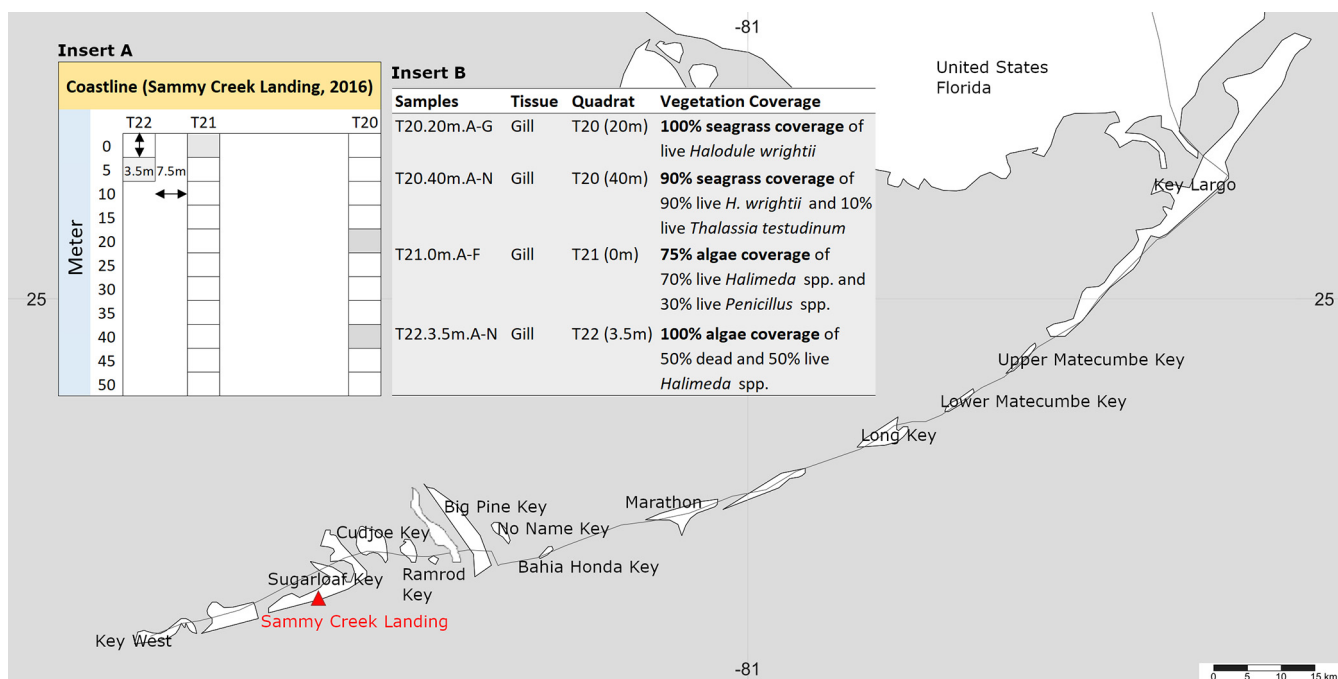


FIG 1 Map showing location of the sampling site at Sammy Creek Landing in Florida, USA. *Ctena orbiculata* analyses focused on specimens collected from four quadrats (shaded cells in insert A: T20 20 m and 40 m, T21 0 m, and T22 3.5 m) that were covered predominantly with either seagrass or algae (insert B). Map is from SimpleMapppr (92).

from *Codakia orbicularis* (9) and “*Ca. Thiodiazotropha endoloripes*” from *Loripes orbiculatus* (syn = *Loripes lucinalis*) (7), as well as for the clade C endosymbiont from mangrove-dwelling *Phacoides pectinatus* (8), have been investigated using omics approaches. However, limited attention was given to species- and strain-level diversity among the endosymbiont populations. Information about endosymbiont species- and strain-level diversity will be useful for interhost and interpopulation comparisons and could provide new insight into host-symbiont association patterns and possibly biogeographical or environmental drivers of diversity among free-living bacteria in the environment, prior to being acquired by the host or becoming part of the gill microbiome.

In this study, we focused on characterizing the taxonomic, genetic, and functional composition of endosymbiont communities within *Ctena orbiculata* (Montagu, 1808) living sympatrically with at least five other lucinid species in carbonate tidal flat sediment at Sammy Creek Landing, Sugarloaf Key, FL (USA). We selected *C. orbiculata* as the main study organism because it dominated the community. The primary goal was to investigate possible influences of environmental and spatial factors, such as occupation of seagrass- or alga-covered sediment, on endosymbiont diversity, host-symbiont functions, and strain-level diversity by comparing symbionts from multiple individual hosts of the same species. We used *C. orbiculata* gill microbiomes and metagenomes to generate bacterial taxonomic profiles and metagenome-assembled genomes (MAGs) that could test the hypothesis that strain-level *C. orbiculata* endosymbiont diversity exists within a population. Prior research had not been at a sufficiently high genetic resolution to uncover this level of endosymbiont diversity. We also used metatranscriptomic analyses to infer host-symbiont gene expression and to identify differentially expressed genes across *C. orbiculata* endosymbiont taxa and the environment.

RESULTS

Site characterization. A volume of nearly 3 m³ of carbonate sediment was hand dug and hand sieved from 13 quadrats covered with either seagrass or algae (Fig. 1; see also Table S1 in the supplemental material) to reveal a diverse lucinid community that averaged 45.5 live lucinids per m³, predominately from the top 30 cm of sediment. We

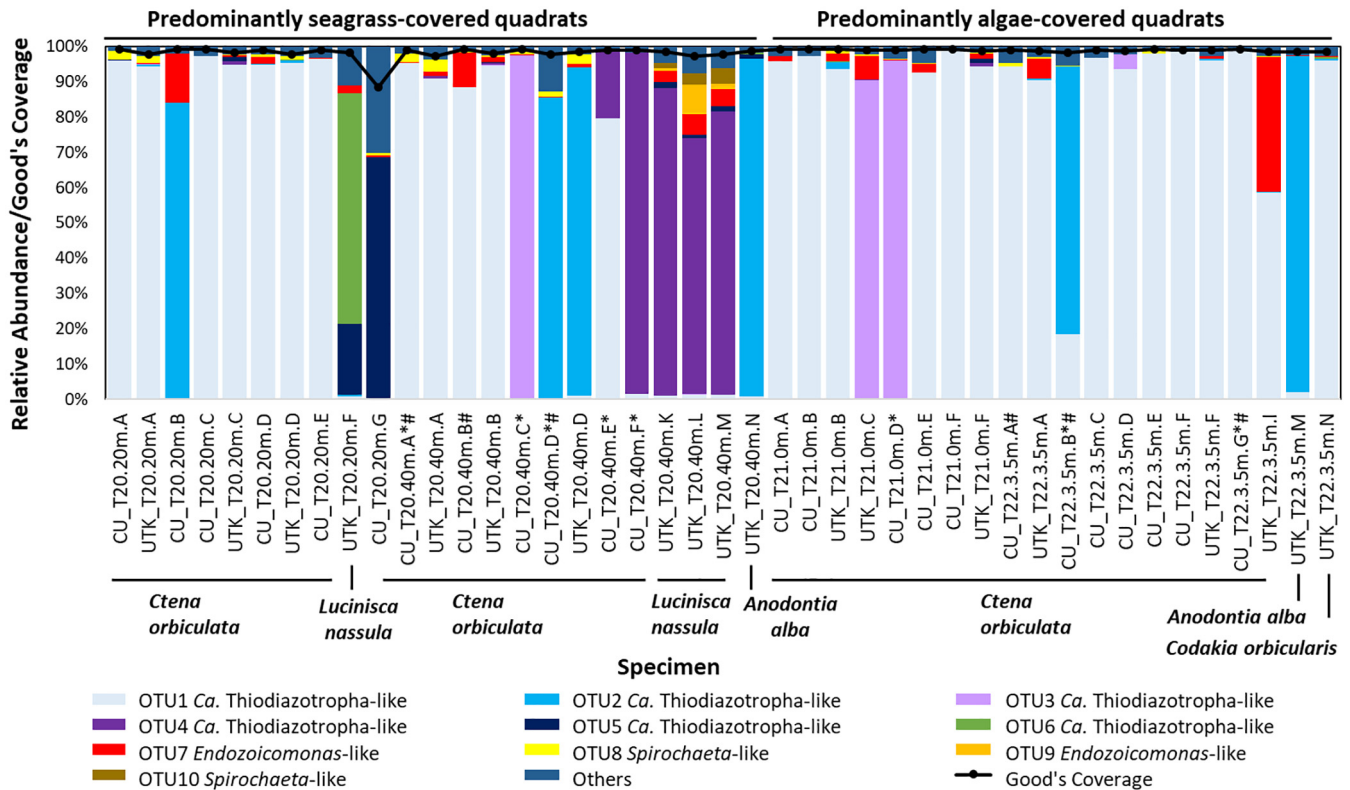


FIG 2 Relative abundances and Good's coverage of subsampled bacterial OTUs identified in lucinid gill specimens collected from Sammy Creek Landing, FL, USA. CU and UTK indicate specimens sequenced by Clemson University and University of Knoxville—Tennessee groups, respectively. Asterisks denote specimens also used for metagenomic sequencing, and pound signs denote specimens used for metatranscriptomic sequencing.

observed an average of 46.4 live *C. orbiculata* specimens from the site quadrats ($n = 13$), 22.3 live *Codakia orbicularis* specimens, 6.2 live *Luciniscia nassula* specimens, and 4.1 live *Anodontia alba* specimens (Table S1). A few live individuals of *Parvilucina pectinella* (1.5) and *Radiolucina amianta* (0.8) were also recovered at the site. Lucinids were encountered from sediment that had a polymodal grain size distribution of very poorly sorted to poorly sorted coarse sand to gravelly sand with an average of 3.3% organic carbon content, regardless of sediment depth. Seagrass species encountered in the quadrats included *Halodule wrightii* (shoal grass), *Syringodium filiforme* (manatee grass), and *Thalassia testudinum* (turtle grass), as well as rhizophytic calcareous algae, such as *Penicillus* spp., *Halimeda* spp., other green algae, and the red algae *Goniolithon* spp. (Table S1). Porewater dissolved sulfide concentrations ranged from $<30 \mu\text{mol/liter}$ to 2.9 mmol/liter, and dissolved oxygen concentrations were lower ($\leq 31 \mu\text{mol/liter}$) than ocean water samples for all sampled quadrats (Table S1). Dissolved methane concentrations were generally higher near the shoreline, with the highest concentration being 2.18 $\mu\text{mol/liter}$ from the same quadrat as the highest sulfide measurement.

Gill microbiome diversity. From the 13 quadrats, four were chosen for detailed examination of lucinid and symbiont diversity based on seagrass or alga coverage (Fig. 1); two quadrats were dominated by *Halodule wrightii* and two others by *Halimeda* spp. To our knowledge, a potential association between lucinids and calcareous green algae has not been established previously. The V4 region of the 16S rRNA gene was sequenced from a total of 36 *C. orbiculata* gill samples retrieved from the four quadrats, as well as from three *L. nassula* gill samples, two *A. alba* gill samples, and one *Codakia orbicularis* gill sample. Of these hosts, 10 *Ctena orbiculata* gill samples were dissected from the same bivalves but processed and sequenced at two different institutions (see Materials and Methods), thus serving as technical replicates (Fig. 2). Sequences were clustered into operational taxonomic units (OTUs) at 99% sequence identity (26) and

showed, on average, $98\% \pm 2\%$ Good's sequencing coverage (27). Taxonomic classification of resulting OTUs against the Silva v132 (28) database at 90% bootstrap confidence revealed six coexisting "*Candidatus Thiodiazotropha*"-like OTUs (OTU1 to OTU6) present at $>60\%$ relative abundances in at least one gill sample from the mixed lucinid community (Fig. 2). OTU1 dominated the gills of 18 of 26 *C. orbiculata* individuals (average relative abundance of $93\% \pm 8\%$) and a single *Codakia orbicularis* individual from the site (99% relative abundance; Fig. 2). The representative sequence for OTU1 was also 100% identical to sequences from two *Codakia orbicularis* individuals previously found in the Bahamas (Fig. S1) (7). OTU2 was predominant in the gills of three *Ctena orbiculata* individuals at $85\% \pm 7\%$ average relative abundance and two *A. alba* individuals at $96\% \pm 0.3\%$ average relative abundance, while OTU3 dominated the gills of three *C. orbiculata* individuals at $95\% \pm 4\%$ average relative abundance (Fig. 2). The OTU3 representative sequence matched the previously sequenced V4 region of the 16S rRNA gene from *L. nassula* off Guadeloupe (22) (Fig. S1). OTU4 dominated the gills of three of four *L. nassula* individuals ($80\% \pm 7\%$ average relative abundance) and one *C. orbiculata* individual (97% relative abundance) but was also detected at 19% relative abundance in another *C. orbiculata* individual and $0.6\% \pm 0.4\%$ relative abundance in six additional *C. orbiculata* individuals (Fig. 2). The representative sequence for OTU4 was identical to sequences retrieved from *P. pectinella* off Guadeloupe (GenBank accession no. [MK346268](#)) and *L. nassula* from Lemon Bay, FL, USA (29) (Fig. S1). OTU5 occurred at 69% relative abundance in the gills of one *C. orbiculata* individual and at $1\% \pm 4\%$ average relative abundances in 17 other individuals (Fig. 2). The OTU distribution did not follow any clear spatial trend. For instance, high relative abundances of OTU1 to OTU3 were identified in gill specimens from both seagrass- and alga-covered quadrats, and OTU4 was detected at high relative abundances ($>50\%$) in gill specimens from a seagrass-covered quadrat (T20 at 40 m) but low relative abundances in the other three quadrats (Table S1). Incidentally, as previously observed in studies on lucinid symbiont diversity (8, 30–32), *Endozoicomonas*-like (order *Oceanospirillales*) and *Spirochaeta*-like bacterial OTUs were also present in lucinid gill tissues from this site (discussed in Text S1).

Metagenomic sequencing of the gills from eight *C. orbiculata* specimens, which were dominated by "*Ca. Thiodiazotropha*"-like OTU1 to OTU4, yielded four OTU-specific clusters of gammaproteobacterial metagenome-assembled genomes (MAGs) (Fig. 3 and Table 1). 16S rRNA gene sequences annotated in OTU1- to OTU4-related MAGs shared 100% identity in their V4 regions with corresponding OTU sequences derived from the same gill specimens. Phylogenetic analyses using the 16S rRNA gene (Fig. S1) and eight single-copy marker genes (Fig. 3A) grouped these MAGs with other clade A thioautotrophic lucinid endosymbionts with OTU-specific clustering. MAGs within each of the four OTU-specific clusters shared $>99\%$ pairwise average nucleotide identity (pANI) and average amino identity (pAAI) with each other and were most similar to the representative MAG of "*Ca. Thiodiazotropha endolucinida*" (9) (Fig. 3B). Species classification of the MAGs, based on the 93% to 95% pANI and 85% to 90% pAAI boundaries proposed by Rodriguez-R. and Konstantinidis (33), showed that the OTU1- and OTU3-related MAGs, which shared $91\% \pm 0.2\%$ pANI and $93\% \pm 0.06\%$ pAAI to each other, were likely different strains of the same species (Fig. 3B). However, OTU1 and OTU3 likely represent a species separate from "*Ca. Thiodiazotropha endolucinida*" ($71\% \pm 5\%$ pANI; $83\% \pm 0.1\%$ pAAI), OTU2 ($80\% \pm 0.7\%$ pANI; $83\% \pm 0.2\%$ pAAI), and OTU4 ($79\% \pm 0.8\%$ pANI; $83\% \pm 0.2\%$ pAAI) (Fig. 3B). OTU2-related MAGs and OTU4-related MAGs shared $81\% \pm 1\%$ pANI and $85\% \pm 0.4\%$ pAAI with each other and $75\% \pm 1\%$ pANI and $85\% \pm 0.2\%$ pAAI, and $73\% \pm 1\%$ pANI and $95\% \pm 0.08\%$ pAAI, respectively, with the representative "*Ca. Thiodiazotropha endolucinida*" MAG (Fig. 3B). Therefore, OTU2, OTU4, and "*Ca. Thiodiazotropha endolucinida*" could be considered different strains of the same species.

Metagenomic read coverage profiles of each representative OTU-specific MAG, bacterial replication rates estimated by iRep (34) from MAG data, and percentages of metatranscriptomic reads mapped to protein-encoding genes of each representative

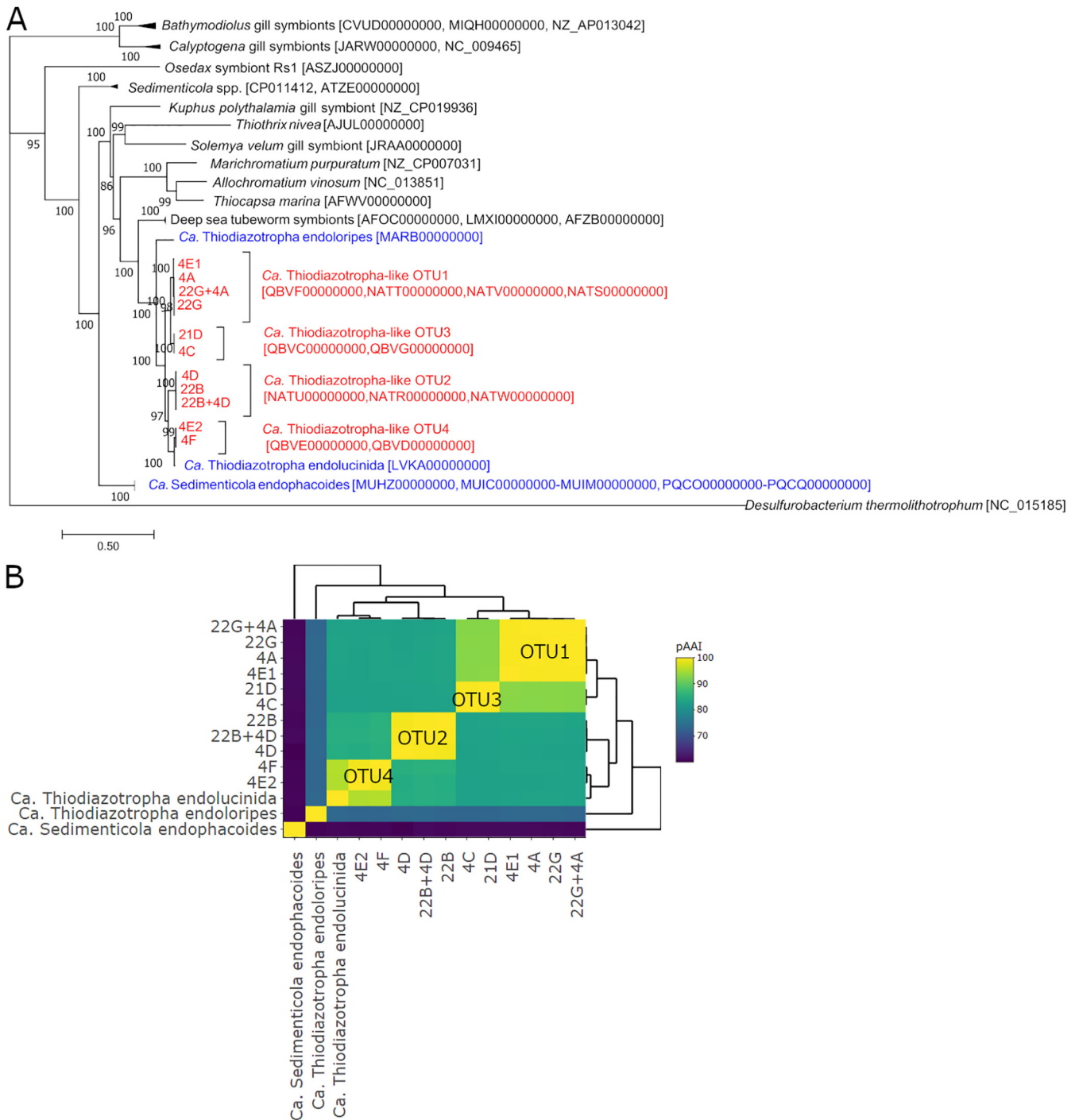


FIG 3 (A) Phylogenomic tree (outgroup *Desulfurobacterium thermolithotrophum*) of *C. orbiculata* symbiont MAGs in this study in relation to lucinids (blue), other bivalves, tubeworm symbionts, and free-living bacteria using eight single-copy marker genes (*dnaG*, *nusA*, *pgk*, *rplS*, *rpsE*, *rpsK*, *rpsM*, and *smgB*). (B) Pairwise AAI comparisons between *C. orbiculata* symbiont MAGs and other lucinid symbiont MAGs. GenBank (88) accession numbers in panel A are indicated in brackets. Tree nodes in panel A show approximate likelihood-ratio test (aLRT) SH-like support values (89), and the scale bar indicates 0.5 substitution per site.

OTU-specific MAG were generally consistent with relative abundance patterns of their corresponding 16S rRNA gene OTU (Fig. 4). The only exception was OTU2-dominated gill metatranscriptome 22B from quadrat T22 (3.5 m), which showed higher percentages of reads mapped to OTU1 than to OTU2 (Fig. 4C). Symbiont-specific gill transcriptomes of OTU1-/OTU3-dominated specimens clustered together with an 0.9 ± 0.07 average pairwise Pearson correlation coefficient (PCC), while the OTU2-dominated

TABLE 1 Features of MAGs recovered from *C. orbiculata* gill specimens^a

Categorized species/strain and quadrat	MAG(s)	No. of PE reads (million)	Size (Mb)	No. of contigs	No. of PEGs	% G+C	<i>N</i> ₅₀ (kb)	Completeness by method:			% strain heterogeneity	MAG quality (8)
								CheckM (9)	BUSCO (10)	% contamination		
OTU1												
T22 (3.5 m)	22G	0.5	4.0	235	3,718	56	26	97	94	2	0	High
T20 (40 m)	4A	0.5	3.9	350	3,638	56	16	94	89	2	0	High
Mixed	22G + 4A	1	4.3	182	3,944	56	36	98	96	2	17	High
OTU3												
T20 (40 m)	4E1	5.8	4.2	122	3,833	56	50	98	96	3	33	High
T20 (40 m)	4C	6.2	4.6	42	4,070	57	211	98	94	2	20	High
T21 (0 m)	21D	5.1	4.5	51	4,049	58	139	98	95	2	0	High
OTU2												
T22 (3.5 m)	22B	0.3	4.0	309	3,700	54	19	97	88	4	28	Medium
T20 (40 m)	4D	0.5	3.4	656	3,127	53	6	84	69	2	0	Medium
Mixed	22B + 4D	0.8	4.1	193	3,729	53	34	98	96	3	8	Medium
OTU4												
T20 (40 m)	4E2	5.8	4	593	3,730	53	9	91	77	4	37	Medium

^aAbbreviations: PE, paired end; PEGs, protein-encoding genes.

symbiont transcriptome 4D from quadrat T20 (40 m) and OTU4-dominated symbiont transcriptome 4F from quadrat T20 (40 m) appeared to be outliers sharing <0.4 PCC with the other specimens (Fig. 5). Symbiont OTU-specific patterns were not observed across the entire gill metatranscriptomes (average 0.7 ± 0.4 PCC between samples) or another subset of Mollusca-related transcriptomes (average 0.8 ± 0.06 between samples). Host 18S rRNA, 28S rRNA, and mitochondrial cytochrome *b* (*cytb*) gene sequences extracted from unbinned *C. orbiculata* gill metagenomes clustered unambiguously with reference sequences from *C. orbiculata* (Fig. S2), thereby confirming the host taxonomy of these specimens.

Core symbiont functions. Pangenomes of “*Ca. Thiodiazotropha*”-like MAGs were predicted by Rapid Annotation using Subsystem Technology (RAST) (35) to share ~62% gene and ~83% subsystem content. As noted by Lim et al. (8), gene and subsystem annotations were based on incompletely sequenced and annotated MAGs. As such, the numbers of shared genes and subsystems presented here are imprecise estimates that cannot account for missing, unbinned, or unclassifiable genes or for incomplete pathways and potential strain/cross-species contamination of the MAGs. Moreover, limitations of host-symbiont metatranscriptomic analyses also apply (8).

Nevertheless, even with incompletely annotated MAGs, the *C. orbiculata* symbionts showed high expression of a carbon storage regulator (103 ± 97 average trimmed mean of M-value [TMM] normalized transcripts per million [TPM]), thioautotrophy-related form I_{aq} RuBisCO (average 18 ± 19 TPM), and adenylylsulfate reductase subunit A (average 15 ± 12 TPM), which were among the 35 most abundant transcript clusters (loosely equivalent to genes) in the symbiont transcriptomes (Fig. 6). Specifically, MAGs of OTU1, OTU3, and “*Ca. Thiodiazotropha endoloripes*” (7) encoded and expressed form I_{aq} RuBisCO, whereas OTU2, OTU4, and “*Ca. Thiodiazotropha endolucinida*” (9) encoded and expressed form I_{aq} and form II RuBisCO (Fig. S3). Form II RuBisCO was expressed only in the OTU2-dominated gill specimen 4D from the seagrass quadrat T20 (40 m) at 0.205 TPM and was not identified in the unbinned metagenomes of OTU1- and OTU4-dominated gill specimens. For contrast, only form II RuBisCO was predicted in the mangrove-associated *P. pectinatus* symbiont species, “*Candidatus Sedimenticola endophacoides*” (8). From the *C. orbiculata* MAGs, many stress-related symbiont transcript clusters encoding multiple heat shock proteins (average 164 ± 220 TPM), the antioxidant glutathione peroxidase (average 66 ± 93 TPM), envelope stress-associated RNA polymerase sigma factor RpoE (average 37 ± 67 TPM) (36), a cold shock domain-

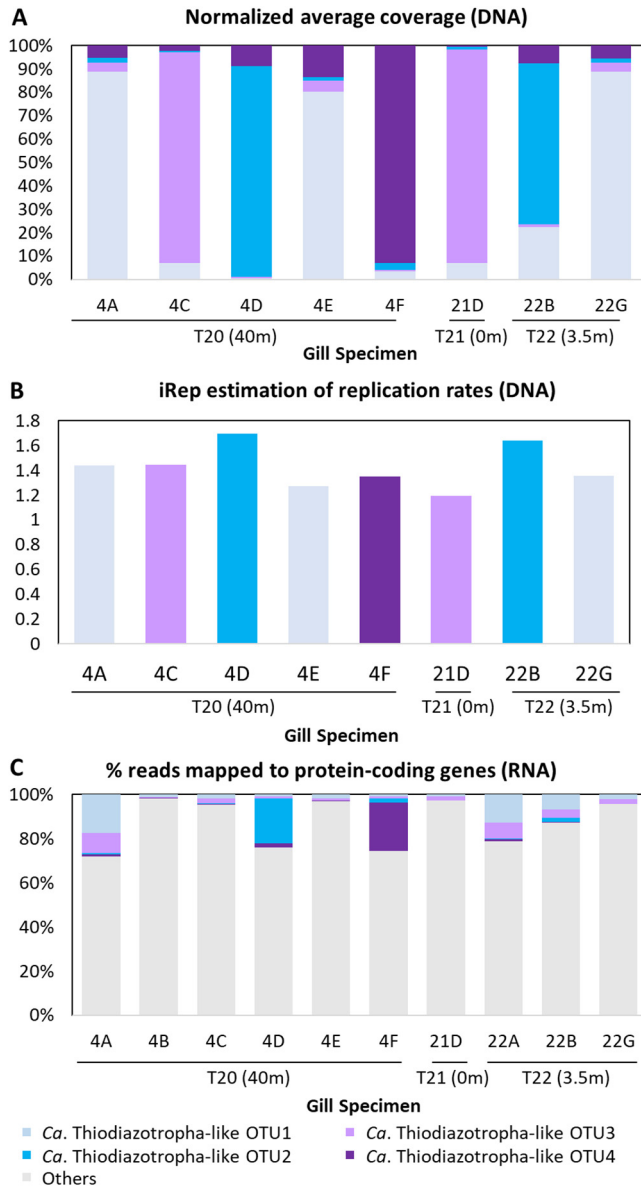


FIG 4 (A) Percent average coverage depths normalized by MAG size. (B) iRep (34) estimation of replication rates. (C) Percent metatranscriptomic reads of each sequenced gill specimen from specific quadrats mapped to each representative taxon-specific MAG. Only bars with an ≥ 0 estimated replication rate are shown in panel B.

containing protein (average 34 ± 31 TPM), heat stress-associated RpoH (37), and the stringent response-associated RNA polymerase binding protein DksA (38) were abundant (Fig. 6). In addition to thioautotrophy and mixotrophy, other functions common to the *C. orbiculata* symbiont species and other previously characterized thioautotrophic lucinid symbiont species (7–9) included hydrogenotrophy (average 1 ± 2 TPM), ammonia uptake (average 0.4 ± 0.7 TPM), denitrification (average 0.5 ± 1 TPM), assimilatory nitrate reduction (average 0.03 ± 0.04 TPM), and diazotrophy (average 0.08 ± 0.1 TPM) (Fig. S3a). Genetic evidence for urea hydrolysis in *C. orbiculata* symbionts was weak (Text S1). The *C. orbiculata* symbionts expressed flagellum-related genes (average 0.9 ± 5 TPM) and pilus-related genes (average 1 ± 7 TPM), as well as genes associated with phosphate uptake (average 0.3 ± 0.8 TPM), polyphosphate utilization (average 0.2 ± 0.6 TPM), and iron uptake (average 0.2 ± 0.4 TPM). Biosynthetic genes for all 20 essential amino acids and vitamins B₁, B₂, B₆, B₇, and B₉ and type I, II, and VI

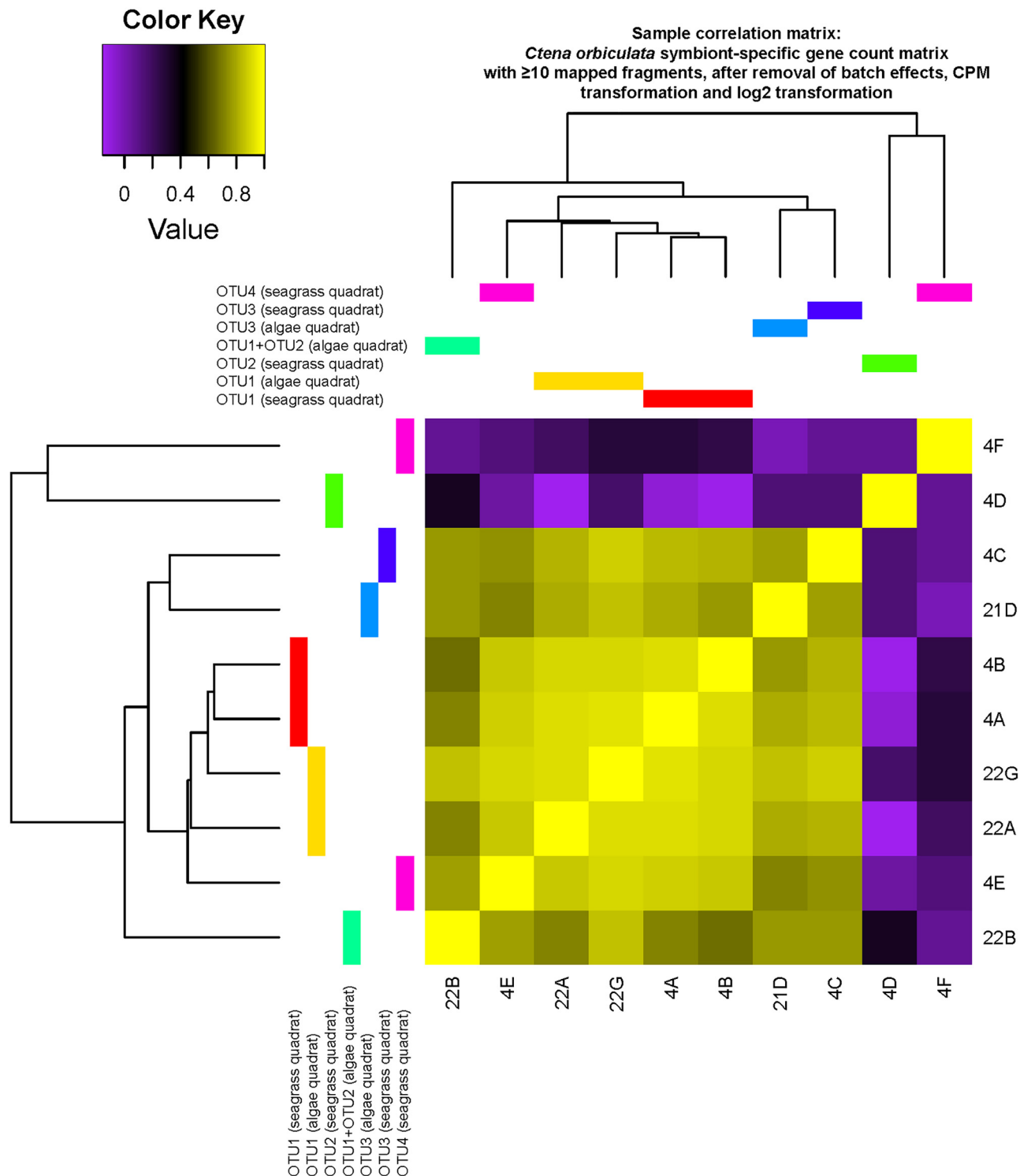
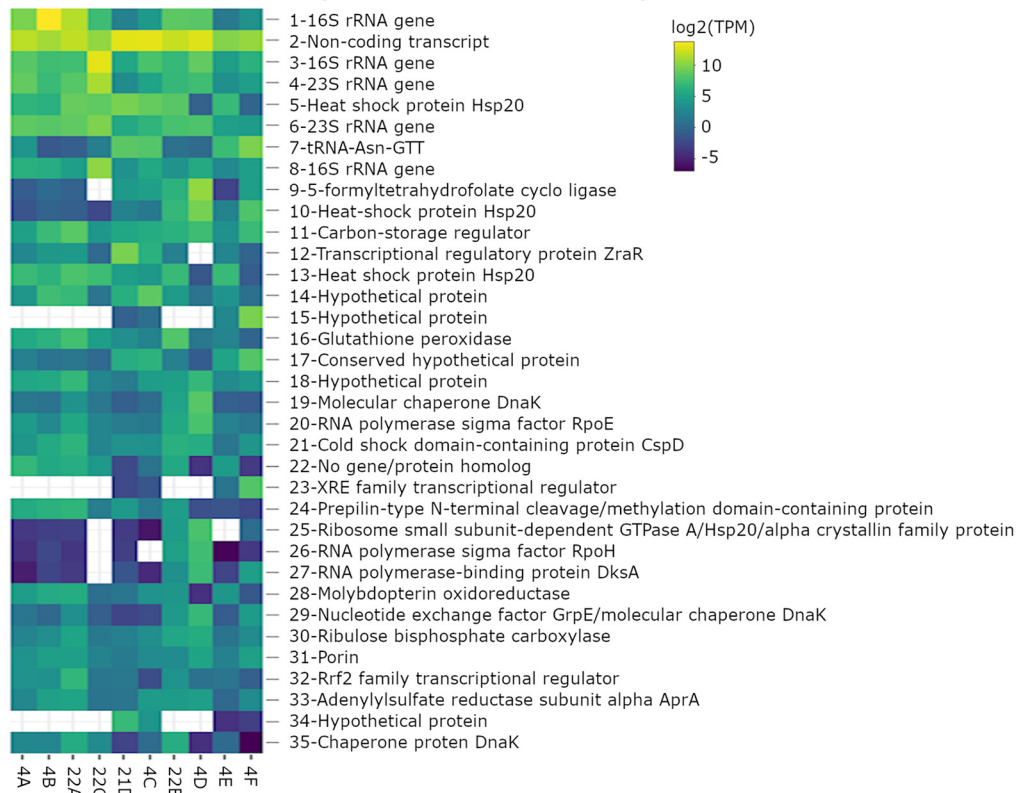


FIG 5 Heat map of pairwise Pearson correlations across gill specimens, based on the number of assembled transcripts mapped to genes in symbiont transcriptomes extracted from the metatranscriptomic assembly. The count matrix was processed to filter out genes with < 10 mapped fragments and to eliminate batch effects and was normalized to log₂ counts per million (CPM).

secretion system genes were also identified in symbiont MAGs and transcriptomes. *Ctena orbiculata* symbionts also encoded and expressed genes for the valine-glycine repeat protein G (VgrG; average 0.7 ± 1 TPM) but not hemolysin-coregulated protein (Hcp) and VasL, which is exclusive to the type VI secretion system 2 gene cluster (39).

A 35 most abundant transcript clusters in *Ctena orbiculata* symbionts



B 35 most abundant protein-coding transcript clusters in *Ctena orbiculata* gill metatranscriptomes

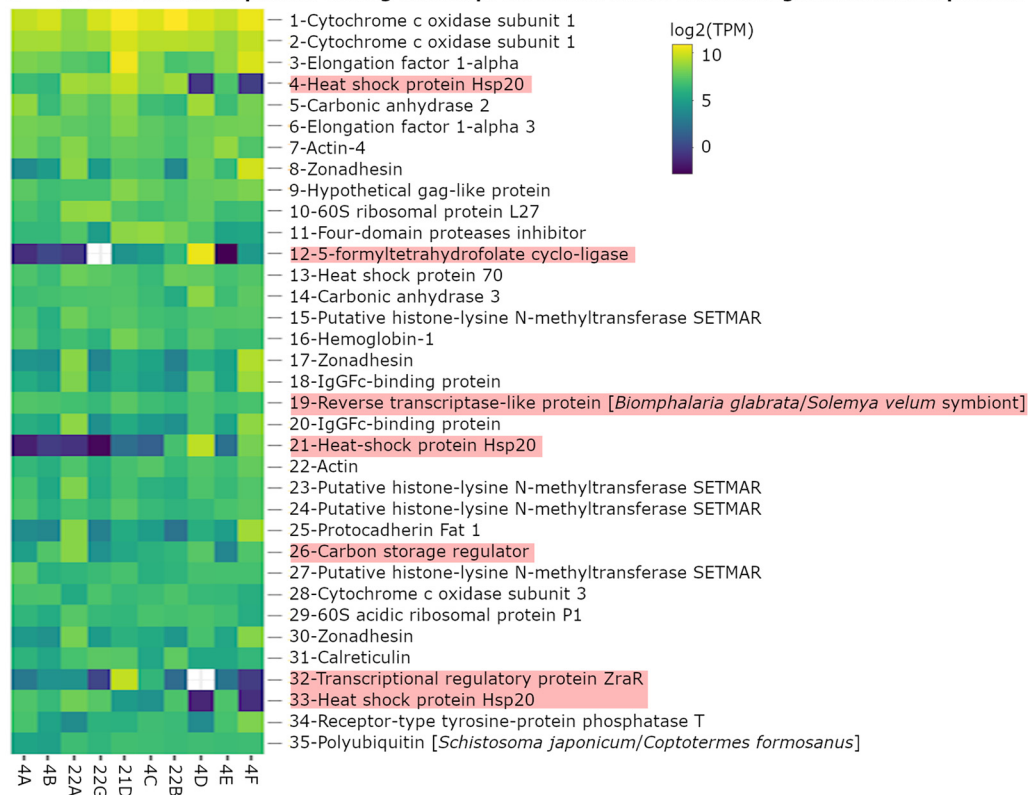


FIG 6 Log₂-transformed trimmed mean of M-values (TMM)-normalized TPM of gene products of the 35 most abundantly expressed transcript clusters mapped to *C. orbiculata* symbionts (A) and protein-encoding transcript clusters in sequenced gill metatranscriptomes (B). Bacterium-related transcripts in panel B are highlighted in pink.

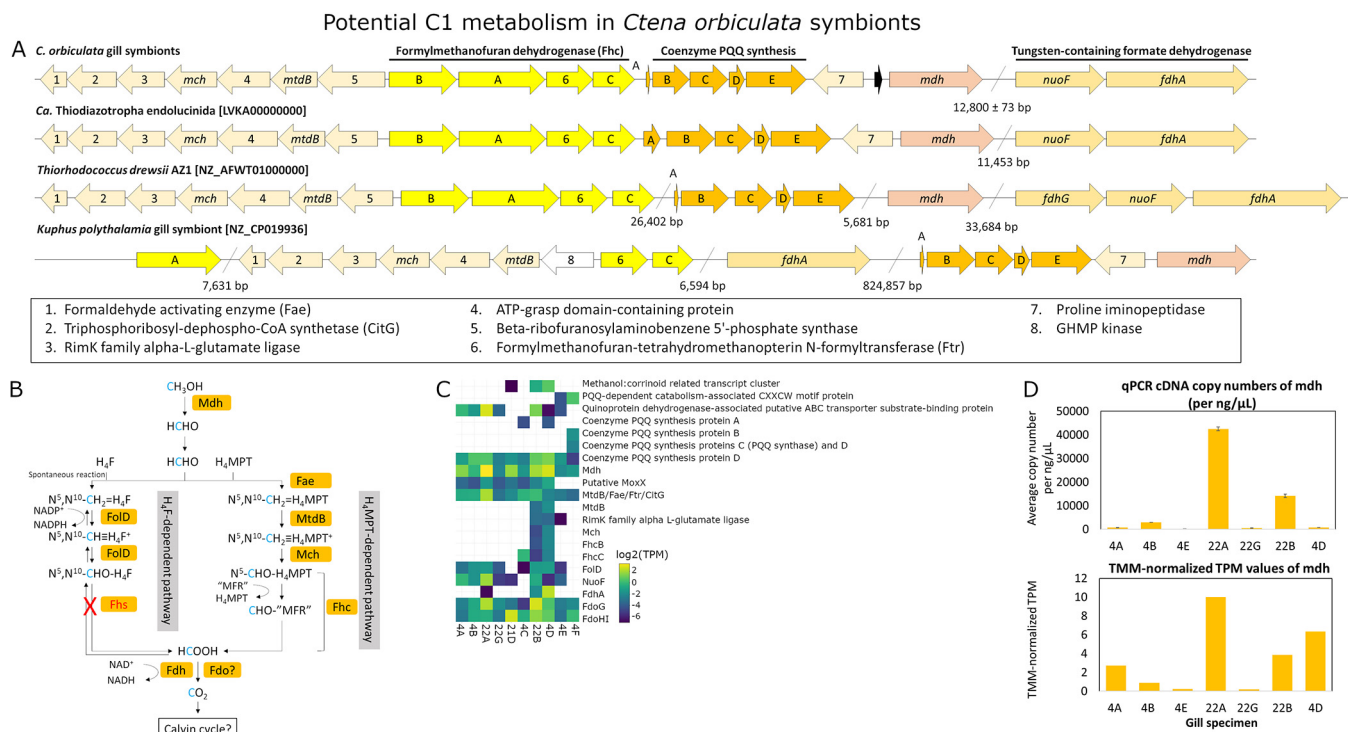


FIG 7 (A) Conserved gene clusters. (B) Proposed pathways modified from references 90 and 91. (C) TMM-normalized \log_2 TPM. (D) qPCR copy numbers and TMM-normalized TPM values of methanol dehydrogenase and/or other C₁ oxidation genes in *Ctena orbiculata* symbiont species. Colored arrows in panel A depict genes conserved in at least two species, and the black and white arrows represent genes encoding hypothetical and nonconserved proteins, respectively. Abbreviations: Mch, methenyl-tetrahydromethanopterin cyclohydrolase; MtdB, NAD(P)-dependent methylene-tetrahydromethanopterin dehydrogenase; Mdh, pyrroloquinoline-quinone (PQQ)-dependent methanol dehydrogenase; NuoF, NADH-quinone oxidoreductase subunit F; Fdh, NAD-dependent tungsten-containing formate dehydrogenase; RimK, ribosomal protein S6 modification enzyme; GHMP, galacto-, homoserine, mevalonate, and phosphomevalonate; H₄F, tetrahydrofolate; Fold, bifunctional methylene-H₄F dehydrogenase/methenyltetrahydrofolate cyclohydrolase; Fhc, formyltransferase/hydrolase complex; Fdo, formate dehydrogenase O; Fae, formaldehyde activating enzyme; “MFR,” postulated methanofuran analogue; Fhs, formyl-H₄F synthetase; ABC, ATP-binding cassette; MoxX, methanol utilization control regulatory protein.

In addition to thiotrophy and hydrogenotrophy-related genes, a C₁ oxidation gene cluster encoding proteins involved in pyrroloquinoline quinone (PQQ) synthesis (average 0.2 ± 0.6 TPM), PQQ-dependent methanol oxidation (Mdh; average 3 ± 3 TPM), and tetrahydromethanopterin (H₄MPT)-dependent formaldehyde oxidation (average 0.2 ± 0.6 TPM) was conserved in all sequenced *C. orbiculata* symbionts and “*Ca. Thiodiazotropha endolucinida*” (8) (Fig. 7). Downstream of this gene cluster, another formate oxidation gene cluster encoding NADH-quinone oxidoreductase subunit F and formate dehydrogenase alpha subunit (FdhA) was predicted in all *C. orbiculata* symbionts, “*Ca. Thiodiazotropha endolucinida*” (9), and “*Ca. Thiodiazotropha endoloripes*” (7). Phylogenetic analyses of Mdh and FdhA protein sequences showed OTU-specific clustering patterns across *C. orbiculata* symbionts (Fig. S4 and S5 and Text S1) consistent with the 16S rRNA gene tree (Fig. S1) and phylogenomic tree (Fig. 3A). These sequences were most closely related to each other and more distantly associated with the giant Teredinidae bivalve *Kuphus polythalamia* (40) and other free-living bacterial species (Text S1). Two sets of qPCR primers targeting Mdh from OTU1 and OTU2 were designed to amplify DNA and cDNA from gill specimens (Table S2), and the qPCR cDNA copy numbers of Mdh were generally consistent with TPM values observed in five out of seven amplified gill specimens (Fig. 7D). Other genes potentially related to C₁ oxidation were also annotated in MAGs and/or transcriptomes of *C. orbiculata* symbionts (Text S1). C₁ assimilation genes in the ribulose monophosphate (RuMP) pathway, and four out of 10 key genes (serine hydroxymethyltransferase, malyl coenzyme A lyase [malyl-CoA-lyase], malate dehydrogenase, and enolase) in the serine-glyoxylate cycle (41), were identified in the symbiont MAGs. These four genes, as well as 11 additional

accessory genes assigned by RAST (35) to the serine-glyoxylate cycle subsystem, were also predicted in other carbon-related pathways, including biosynthesis, glycolysis, photorespiration, tricarboxylic acid cycle, glyoxylate cycle, polyhydroxybutyrate metabolism, acetyl-CoA fermentation to butyrate, and phenylalkanoic acid degradation.

Core host functions. Gill metagenomic and metatranscriptomic data also provided information on highly expressed host functions. Carbonic anhydrase transcript clusters mapped to molluscan species (average 231 ± 149 TPM) and the sea lamprey *Petromyzon marinus* (average 140 ± 86 TPM), together with a lucinid-associated hemoglobin 1 transcript cluster (average 124 ± 60 TPM), were among the 20th most abundant protein-encoding transcripts in the gill metatranscriptomes, respectively (Fig. 6B). In contrast to hemoglobin 1, lucinid-associated hemoglobins 2 (average 0.2 ± 0.7 TPM) and 3 (average 0.8 ± 2 TPM) were expressed at much lower levels. Two Mollusca-related transcript clusters encoding IgG Fc-binding proteins (average 117 ± 144 TPM) were also among the 25th most abundantly expressed in the gills (Fig. 6B). This has not yet been observed in other lucinid species but may contribute to mucosal defense (42) or facilitate initial symbiont selection of tightly aggregated symbionts as in the *Euprymna-Vibrio* symbiosis (43). Among lysozyme-associated transcripts in *C. orbiculata* (average 0.9 ± 2 TPM), presumably expressed to enable microbiome selection and/or digestion (8, 44), one molluscan-related transcript cluster encoding lysozyme 3 was the most highly expressed (average 4 ± 2 TPM). Bivalve-related transcript clusters homologous to urease (average 1 ± 3 TPM), urease accessory proteins (average 0.2 ± 0.2 TPM), and urease transporters (average 0.2 ± 0.5 TPM) were also identified in all gill metatranscriptomes.

Symbiont species/strain differences. In addition to interspecies differences in the forms of RuBisCO identified, *C. orbiculata* symbiont MAGs and transcriptomes showed very little interstrain and interspecies variation of complete or nearly complete metabolic pathways. For aerobic respiration, *C. orbiculata* symbionts and other clade A lucinid symbionts (7, 9) potentially utilize *cbb3* (average 4 ± 5 TPM in the former) and *aa3* terminal oxidases (average 5 ± 9 TPM). Furthermore, OTU2-related MAGs and transcriptomes contained genes for cytochrome *bd* ubiquinol oxidase (average 0.5 ± 0.4 TPM) that were also detected in the unbinned metagenomic assembly and metatranscriptome of OTU4-dominated gill specimen 4F from the seagrass-covered quadrat T20 (40 m) at 0.02 TPM, as well as the metatranscriptome of OTU3-dominated gill specimen 4C from quadrat T20 (40 m) at 0.3 TPM. *Ctena orbiculata* symbionts also likely use distinct types of clustered regularly interspaced short palindromic repeats (CRISPR)-associated genes (Text S1).

Differential expression (DE) analyses on symbiont-related genes using four DE algorithms showed <20 total DE transcript clusters ($P < 0.05$, ≥ 2 -fold change) for OTU2-OTU3, OTU2-OTU4, and OTU3-OTU4 community comparisons (Fig. S6). On the other hand, OTU1-OTU3 comparisons showed four total upregulated and 88 downregulated genes in OTU1-dominated communities, whereas OTU1-OTU2 comparisons showed 751 total upregulated and 403 downregulated genes in OTU1-dominated communities (Fig. S6). OTU1-OTU4 comparisons showed 10 upregulated and 72 downregulated genes in OTU1-dominated communities (Fig. S6). These genes were mainly involved in secretion, stress response, transport, and biosynthesis functions (Text S1).

DE analyses of host-symbiont gene expression across quadrats. Besides taxon-specific clustering patterns that were evident from 16S rRNA gene profiles and sequence content of the MAGs, OTU1-dominated symbiont-specific transcriptomes formed two separate subclusters based on whether specimens were collected from alga-covered and seagrass-covered quadrats (Fig. 2 and 5), although these transcriptomes shared 0.9 ± 0.01 average pairwise PCC with each other. Exploratory DE analyses on these transcriptomes showed only five symbiont-related DE genes predicted by one (DESeq2) (45) of four DE analysis algorithms used. Of these, the dissimilatory sulfite reductase transferase protein DsrC was upregulated in the alga-covered quadrat, but three transcript clusters that were upregulated in the seagrass-covered quadrat encoded hypothetical proteins and contained one transcript cluster homologous to a cell

wall-associated hydrolase from an alphaproteobacterium. Host-related transcripts did not exhibit the same clustering patterns between alga- and seagrass-covered quadrats but instead showed 73 putative DE genes predicted by both DESeq2 (45) and edgeR (46) across OTU1-dominated metatranscriptomes in these quadrats. According to UniProt (47) annotations, these host-related DE genes were involved in a variety of muscle-related, cytoskeletal, cochaperone, transcriptional, translational, and other functions. Notably, host-related transcripts encoding cytochrome *b-c1* complex, mitochondrial succinate dehydrogenase, and mitochondrial sulfide:quinone oxidoreductase (Sqr) were predicted to be upregulated if originating from seagrass-covered quadrats.

DISCUSSION

To date, the taxonomic and functional diversities of lucinid symbiont species remain largely unexplored because, out of >100 identified lucinid species listed in the NCBI database (48), only three gill endosymbionts, each from a different host species, have been comprehensively sequenced (7–9). In spite of previous marker gene-based diversity studies (20, 22, 23, 25), and the recently characterized gill microbiome, metagenome, and metatranscriptome from “*Ca. Sedimenticola endophacoides*” from *P. pectinatus* (8), in-depth investigations into symbiont variation within a single lucinid host population are currently lacking. Our evidence for endosymbiont species- and strain-level taxonomic, genetic, and functional diversity within a single lucinid host expands previously reported findings of strain-level diversity within a single thioautotrophic endosymbiont species (25). Similar functionally homogenous but taxonomically heterogeneous marine symbiont communities have been reported, for example, in the light organs of the squids *Sepioloa affinis* and *Sepioloa robusta*, where closely related *Vibrio fischeri* and *Vibrio logei* were detected at different abundances (49). The *C. orbiculata* gill metatranscriptomic analyses further reveal differentially expressed host and/or endosymbiont genes of different bacterial taxa. Although gill endosymbiont OTUs from *C. orbiculata* shared a high number of core genes and functions, which included a well-conserved and previously undiscovered C_1 oxidation pathway, the discovery of other genetic and functional differences among coexisting “*Ca. Thiodiazotropha*”-like endosymbiont taxa supports our hypothesis that strain- and even species-level endosymbiont diversity can exist within a single host population living under variable environmental conditions. Moreover, because we also identified “*Ca. Thiodiazotropha*”-like OTUs among other sympatric lucinid species, genetic and functional trait similarities with *C. orbiculata* endosymbionts likely exist within other lucinid populations, which emphasizes the importance of future investigations of these chemolithoautotrophic symbiotic systems at broader population, community, and ecosystem levels.

The thioautotrophic *C. orbiculata* endosymbionts shared a high number of common genes and functions, including previously characterized lithoautotrophy, diazotrophy, and potential heterotrophy (7–9), as well as the oxidation of C_1 compounds, including methanol, formaldehyde, and formate. These potential C_1 compound oxidation functions were also discovered in MAGs of “*Ca. Thiodiazotropha endolucinida*” (9) that had been unrecognized and undescribed until our analyses. *Ctena orbiculata* endosymbionts may use C_1 compounds as an energy source because they encoded and expressed formate dehydrogenase O that enables the use of formate as an electron donor during respiration (50). Because there was no substantial genetic evidence for RuMP and serine-glyoxylate C_1 assimilation pathways, we hypothesize that the CO_2 end product of C_1 oxidation for these endosymbionts could be fixed via the autotrophic Calvin-Benson-Bassham cycle, as demonstrated in the diazotrophic alphaproteobacterial *Xanthobacter* strain 25a (51). Additionally, many transcripts involved in temperature, oxidative, envelope, and nutritional stress responses were highly expressed in *C. orbiculata* endosymbionts and likely reflect stresses caused by the external environment or stresses due to intracellular host selection mechanisms (8), the latter being similar to the *Euprymna-Vibrio* symbiotic system (52–54). Defense-related transcripts involved in type I, II, and VI secretion systems, such as colicin-related transcripts, general secretion (Sec)-related transcripts, and twin-arginine translocation (Tat)-related transcripts, may

reduce symbiont-symbiont competition by killing closely related strains (8, 55), as well as contributing to host infection (56, 57). Also, differentially expressed genes for secretion, stress response, transport, and biosynthesis proteins across the *C. orbiculata* endosymbiont taxa may also be due to variable habitat conditions.

For aerobic respiration, *C. orbiculata* endosymbionts and other seagrass-associated lucinid symbionts (7, 9) can potentially use the high-affinity *cbb3*-type and low-affinity *aa3*-type terminal oxidases under low and high oxygen concentrations (58, 59), respectively. Additionally, cytochrome *bd* ubiquinol oxidase, adapted to microaerobic environments (60), was encoded and expressed mainly by the “*Ca. Thiodiazotropha*”-like OTU2. This enzyme may facilitate symbiotic nitrogen fixation via oxygen scavenging and respiratory protection, as demonstrated in other free-living and plant-associated nitrogen-fixing bacteria (61–63), along with glutathione peroxidase that confers similar protective functions by scavenging H_2O_2 , as shown in the legume-*Rhizobium* symbiosis (64). Conversely, RuBisCO form Ia, detected in “*Ca. Thiodiazotropha*”-like OTU1 to OT4, is more efficient than form II, detected in OTU2 and OTU4, at distinguishing between the competing substrates oxygen and CO_2 (65). Differences in aerobic oxidase and RuBisCO forms, as well as highly expressed antioxidant glutathione peroxidase transcripts, indicate that the symbionts experience higher or variable levels of oxygen in their environments, which could be during their intracellular free-living or extracellular host-associated growth stages. Analyses of host-related transcripts revealed 100-fold-higher expression of sulfide-reactive hemoglobin 1 (66) in *C. orbiculata* compared to oxygen-reactive hemoglobins 2 and 3 (66). This is in contrast with previous observations in *P. pectinatus*, where consistently similar high expression levels of hemoglobins 1, 2, and 3 were detected (8). Compared to alga-covered quadrats, *C. orbiculata* host-related transcripts in seagrass-covered quadrats showed candidate upregulated genes that encoded cytochrome *b-c1* complex involved in aerobic respiration and oxidative stress-triggered apoptosis (67), mitochondrial succinate dehydrogenase that connects the tricarboxylic acid cycle to the electron transport chain (68), and mitochondrial Sqr that oxidizes sulfide to thiosulfate (69). Collectively, these findings indicate that complex host-symbiont cooperative regulation of intracellular oxygen and sulfide levels facilitates thioautodiazotrophic processes, which are distinct from the *P. pectinatus* chemolithoautotrophic symbiotic system (8).

Unlike previous studies on Caribbean lucinid symbiont species (25) and *Sepiolo* squid symbioses (70), where species distribution is influenced by host geography and temperature, respectively, we did not uncover extensive spatial controls or apparent nonrandom patterns of strain-level *C. orbiculata* endosymbiont species distribution. The observed endosymbiont diversity from *C. orbiculata* and other sympatric lucinid species could be due to constant symbiont turnover, because adult *C. imbricatula* clams (referred to as *Codakia orbiculata* in reference 21) have been reported to lose their chemosynthetic endosymbionts when starved for sulfide and reacquire endosymbionts from their natural habitat. This behavior points to continuous horizontal symbiont acquisition throughout the life span of this host species (71, 72). However, a recent cross-infection experiment demonstrates that starved *C. imbricatula* (referred to as *Codakia orbiculata* in reference 21) adults with mature bacteriocytes could reacquire only symbiont strains that they initially hosted (25). In contrast, *Codakia orbicularis* juveniles, presumably with naive bacteriocyte precursors, acquire symbionts from purified gill-symbiont sections of their own species, as well as other lucinid species hosting thioautotrophic symbionts with identical 16S rRNA gene sequences (24, 25). On the other hand, starvation-related symbiont loss has not been observed in *Lucina roquesana* (referred to as *Lucina pensylvanica* in references 21 and 73). The contrasting evidence for symbiont acquisition, loss, and reacquisition suggests that such mechanisms could be host species specific in lucinid bivalves (73). Based on our results, it does not appear that a single symbiont species occupies a single host. Instead, a single host may harbor multiple symbiont species and strains. This is likely due to either higher taxonomic symbiont diversity encountered by the host in the environment (20) or less stringent host regulation of symbiont acquisition in the mixed lucinid community (25).

Interhost symbiont transmission could also be a possible reason for the observed symbiont diversity in the mixed lucinid community. However, previous studies on *C. imbricatula* (referred to as *Codakia orbiculata* in reference 21) and *Codakia orbicularis* ruled out the possibility of host-to-host symbiont transfer by showing that adults do not release their thioautotrophic symbionts into the environment (74). In addition, opportunistic host-microbe associations have been proposed for lucinid bivalves (20) and observed in the green macroalga *Ulva australis* (75). Therefore, symbiont acquisition by this mixed lucinid community may be based on random encounters during the juvenile stage, as well as the diversity and distribution of “Ca. Thiodiazotropha” species in this habitat, which are under investigation. Nevertheless, our results suggest that a taxonomically heterogeneous symbiont community, rather than a monospecific, homogeneous symbiont community, exists in some lucinid species.

Overall, our study uncovered remarkable taxonomic, genetic, and functional thioautotrophic gill endosymbiont diversity in *C. orbiculata* and furthers the current understanding of lucinid-symbiont association patterns, physiology, and interactions. Despite the small sample size and replication limitations that potentially affect the statistical significance of DE analysis, as well as the lack of pure symbiotic monocultures, our findings highlight the intriguing, poorly understood complexity of lucinid-bacterium chemolithoautotrophic symbioses and generate a range of new testable hypotheses to evaluate the establishment, persistence, stability, and distribution of symbiont communities within hosts and their environment. Future studies to understand symbiont taxonomy, intracellular spatial distribution, functional diversity, and host-symbiont specificity across environmental gradients should include cross-infection experiments, imaging experiments involving fluorescence *in situ* hybridization, controlled aquarium experiments, and large-scale field studies coupled with -omics analyses. This work also proposes future in-depth investigations on C₁ metabolism in thioautotrophic lucinid symbionts and three-way interactions between the environment, lucinid hosts, and their symbionts. Additionally, targeted experimental approaches will be useful in examining similarities and differences in phenotypic effects that various symbiont taxa and lucinid hosts exert on each other. In each of the previous -omics studies of lucinid chemolithoautotrophic symbiotic systems, a unique species name for the lucinid endosymbiont has been proposed, such as the two clade A endosymbionts, “Ca. Thiodiazotropha endolucinida” from *Codakia orbicularis* (9) and “Ca. Thiodiazotropha endoloripes” from *Loripes orbiculatus* (7). For the clade C endosymbiont from the mangrove-dwelling *P. pectinatus* (8), which does not fix nitrogen and instead belongs to the genus *Sedimenticola*, the candidate name for the endosymbiont was justifiably proposed as “Ca. *Sedimenticola* endophacoides” (8). However, based on our analyses here, we think it is too premature to assign a species name for the *C. orbiculata* symbionts. Even if “Ca. Thiodiazotropha endolucinida” is likely appropriate for the OTU2 and OTU4 strains, the OTU1 and OTU3 strains likely belong to a different species, but this species is not specific to *C. orbiculata* or even to lucinid hosts having clade A endosymbionts. Therefore, we contend that future lucinid symbiont taxonomic assignments and classification need to be based on detailed investigations of more lucinid symbionts from all three endosymbiont clades and from different habitats.

MATERIALS AND METHODS

Study area and sediment characterization. Field sampling was done on the carbonate tidal flat at Sammy Creek Landing, on Sugarloaf Key, FL (USA), from 27 June to 1 July 2016. Twelve quadrats were separated by 5 m along two 50-m-long transects (six quadrats each) that ran perpendicular to the shoreline; a 13th quadrat was established 3.5 m away from shore to accommodate equal sampling of seagrass versus benthic green and red algal cover (Fig. 1). The seagrass or algal cover was estimated for each quadrat before hand digging and hand sieving the sediment to uncover lucinids and other infauna. In general, depths of sediment excavation varied, from 0.29 to 0.5 m, and generally stopped at a very coarse, organic-material-rich sediment layer below which lucinids were not recovered. Intermixed with the sediment was abundant road (e.g., concrete and asphalt) and other anthropogenically sourced debris, such as manufactured wood, roofing material, and mixed-use plastic, likely due to past storm activity that impacted the shoreline and tidal flat. Methods for geochemical and sedimentological analyses are in Text S1 in the supplemental material.

Sample collection and sequencing. Prior to dissection, all live-collected lucinid specimens were temporarily stored and transported in Whirl-Pak bags (Nasco, Fort Atkinson, WI, USA) at ambient temperature filled with surface water from the habitat (8). Dissection was performed within 30 min or within the same day of collection (explained below), where gill and foot tissues were separated from other body tissues and preserved in RNAlater (8). Dissected gill tissues were divided for molecular and sequence analyses between Clemson University (CU; Clemson, SC, USA) and University of Tennessee—Knoxville (UTK; Knoxville, TN, USA) such that, for each specimen, one fixed gill tissue went to each institution or both gill tissues went to UTK. Valves and the remaining preserved tissues were archived and cataloged at the Museum of Geology at the South Dakota School of Mines and Technology (Rapid City, SD, USA). This study focused on specimens from four of 13 quadrats that were predominantly covered by either seagrass or algae: T20 (20 m), T20 (40 m), T21 (0 m), and T22 (3.5 m) (Fig. 1). *Ctena orbiculata* specimens from these four quadrats used for 16S rRNA gene, metagenomic, and metatranscriptomic analyses at CU were preserved within 30 min of collection. Nucleic acids extraction, fluorometric DNA/RNA quantification, cDNA synthesis, and 16S rRNA gene library preparation from this collection were performed as described in the work of Lim et al. (8). At CU, the V4 region of the 16S rRNA gene from 24 *C. orbiculata* gill tissues, as well as metagenomic libraries prepared from DNA extracted from eight *C. orbiculata* gill samples using NEBNext dsDNA Fragmentase plus the NEBNext Ultra II DNA library prep kit for Illumina or the NEBNext Ultra II FS DNA library prep kit for Illumina (New England Biolabs, Ipswich, MA, USA), were sequenced on the Illumina MiSeq V2 2-by 250-bp platform (San Diego, CA, USA). RNA extracted from 11 *C. orbiculata* gill samples at CU was prepared for metatranscriptomic sequencing, using procedures in the work of Lim et al. (8), on the Illumina HiSeq 4000 2-by 150-bp platform at the Duke Center for Genomic and Computational Biology (Durham, NC, USA). All library concentrations were quantified with the Qubit dsDNA HS assay (Life Technologies, Austin, TX, USA), and their insert sizes were determined with the Agilent 2100 Bioanalyzer (Agilent Technologies, Santa Clara, CA, USA). Specimens of additional *C. orbiculata* individuals ($n = 3$) and other sympatric lucinid species ($n = 7$) from the same four quadrats were also used for only 16S rRNA gene analysis at UTK. These specimens were preserved within the same day of collection. DNA was extracted from the gill tissues of 12 *C. orbiculata* (including 9 of the gill samples fixed by CU), four *L. nassula*, two *A. alba*, and one *Codakia orbicularis* specimen using methods described in the work of Lim et al. (8). 16S rRNA gene V4 region libraries of these samples were prepared and sequenced by Molecular Research LP (Shallowater, TX, USA) using the Illumina MiSeq V3 2-by 300-bp platform.

Data analyses. 16S rRNA gene sequence reads from CU and UTK were combined, quality trimmed, and processed with MOTHUR v1.41.1 (76) using the pipeline documented in the work of Lim et al. (8). Briefly, all reads were quality trimmed at $Q = 25$ using MOTHUR's `trim_seq` and `remove_seq` commands and processed according to MOTHUR's MiSeq SOP available at https://www.mothur.org/wiki/MiSeq_SOP. OTUs clustered at 99% sequence identity were taxonomically classified using the Silva v132 database (28) with 90% bootstrap confidence. The data set was subsampled to 6,676 sequences, which was the number of sequences in the smallest library. OTU relative abundances and Good's coverage (27) within each sample were calculated using the MOTHUR `get.relabund` and `summary.single` commands, as described in the work of Lim et al. (8). Representative sequences of the 10 most abundant OTUs were obtained using MOTHUR's `get.otu rep` command, which identifies a representative sequence sharing the smallest maximum or average distance (in the event of a tie) to other sequences classified within the same OTU. Reads from all eight metagenomic libraries were trimmed and assembled individually (8). Additionally, two metagenomic libraries of gill specimens dominated by OTU1 and two libraries of gill specimens dominated by OTU2 were coassembled separately. Read mapping, binning, MAG quality assessment, MAG annotation, and ANI and AAI calculations were performed as detailed in the work of Lim et al. (8). Methods for phylogenetic analyses are outlined in Text S1 in the supplemental material. Bacterial replication rates were estimated using the iRep software (34) by mapping metagenomic reads to representative OTU-specific MAGs (22G, 22B + 4D, 21D, and 4F) with $\geq 75\%$ completeness and $\leq 2\%$ contamination, using Bowtie 2 v2.3.4.1 (77) in very sensitive local and dovetail mode and SAMtools v1.7 (78). For metatranscriptomic analyses, a pangenome for each symbiont OTU was created using the method in the work of Lim et al. (8). *De novo* metatranscriptomic assembly, transcript cluster (gene) abundance estimation, count normalization, transcript-to-gene mapping, and transcript annotation were performed using Trinity v2.6.6 (79), Trinotate v3.1.1 (<https://trinotate.github.io/>), and web and local Blast searches (48), as described in the work of Lim et al. (8). For symbiont abundance estimation, trimmed reads were mapped to representative MAGs using the Bowtie 2 (77) `-no-unal -no-mixed -no-discordant -gbar 1000 -end-to-end -k 200` options. Nonchimeric fragments mapped to protein-encoding genes were calculated with featureCounts v1.5.2 (80) using the `-c` and `-p` options. DE and functional gene ontology (GO) enrichment analyses were performed on a raw read count matrix processed with Trinity's `remove_batch_effects_from_count_matrix.pl` script. Batch-removed read counts of transcript clusters mapped to thioautotrophic symbiont MAGs and those with eukaryotic homologs were analyzed separately using DESeq2 (45), edgeR (46), Reproducibility-Optimized Test Statistic (ROTS) (81), voom (82), and GOSeq (83) software incorporated within Trinity. DESeq2 (45) and edgeR (46) rely on the negative binomial distribution for DE analyses but differ in their normalization and statistical testing methods. ROTS uses properties from gene expression data to optimize a modified t statistic that maximizes the overlap of top-ranked genes in group-preserving bootstrapped data sets (81), while voom models the mean-variance relationship of depth-normalized log counts nonparametrically, incorporates it into a precision weight for each individual observation, and then fits a linear model to the weighted data using the *limma* package (84) for DE analyses (82). On the other hand, GOSeq (83) identifies Gene Ontology (GO) (85) terms, extracted from Trinotate's annotations, that are over- and underrepresented in DE gene data sets predicted by each software program. To identify DE genes and

GO terms, a threshold of >2 -fold change and <0.05 false-discovery rate (FDR)-adjusted P value was applied (86), with the latter corresponding to a false-positive rate of 5% among all statistically significant DE genes. Predictions made by these tools were compared using Venny (87). qPCR methods to verify *mdh* gene expression are described in Text S1.

Availability of data and materials. Physical specimen details are available through the iDigBio portal (<https://www.idigbio.org/portal/recordsets/db3181c9-48dd-489f-96ab-a5888f5a938c>). Sequence data were uploaded to NCBI (48) under the BioProject IDs PRJNA377790 (CU) and PRJNA510358 (UTK). Accession numbers are listed in Table S3.

SUPPLEMENTAL MATERIAL

Supplemental material for this article may be found at <https://doi.org/10.1128/mSystems.00280-19>.

TEXT S1, DOCX file, 0.04 MB.

FIG S1, PDF file, 1.6 MB.

FIG S2, TIF file, 0.8 MB.

FIG S3, TIF file, 2.7 MB.

FIG S4, PDF file, 0.8 MB.

FIG S5, TIF file, 0.9 MB.

FIG S6, TIF file, 0.9 MB.

TABLE S1, DOCX file, 0.01 MB.

TABLE S2, DOCX file, 0.01 MB.

TABLE S3, DOCX file, 0.01 MB.

ACKNOWLEDGMENTS

This research was permitted by the Florida Fish and Wildlife Conservation Commission through a Special Activity License (SAL-14-1599C-SR) and the Florida Keys National Marine Sanctuary (FKNMS-2016-056) to A.S.E.

This work is supported through the Dimensions of Biodiversity Program of the National Science Foundation (DEB-1342785 to A.S.E., DEB-1242721 to L.C.A., and DEB-1342763 to B.J.C.).

We thank Kelsie Abrams for help with field work and data collection; Chantelle Fortier for performing DNA extraction and sample analyses; Vincent Richards, Abdullah Abood, and Yirui Chen for assistance with MiSeq sequencing; and Clemson University's Palmetto cluster for allotment of computing resources.

The authors declare no conflict of interest.

REFERENCES

- Dubilier N, Bergin C, Lott C. 2008. Symbiotic diversity in marine animals: the art of harnessing chemosynthesis. *Nat Rev Microbiol* 6:725–740. <https://doi.org/10.1038/nrmicro1992>.
- Taylor JD, Glover EA. 2010. Chemosymbiotic bivalves, p 107–128. *In* Kiel S (ed), *The vent and seep biota: aspects from microbes to ecosystems*. Springer, Dordrecht, Netherlands.
- Taylor JD, Glover EA. 2000. Functional anatomy, chemosymbiosis and evolution of the Lucinidae, p 207–227. *In* Harper E, Taylor JD, Crame JA (ed), *The evolutionary biology of the bivalvia*. Geological Society of London, London, United Kingdom.
- Cavanaugh CM, McKiness ZP, Newton ILG, Stewart FJ. 2006. Marine chemosynthetic symbioses, p 475–507. *In* Dworkin M, Falkow S, Rosenberg E, Schleifer KH, Stackebrandt E (ed), *The prokaryotes*, 3rd ed, vol 1. Springer, New York, NY.
- Duplessis MR, Ziebis W, Gros O, Caro A, Robidart J, Felbeck H. 2004. Respiration strategies utilized by the gill endosymbiont from the host lucinid *Codakia orbicularis* (Bivalvia: Lucinidae). *Appl Environ Microbiol* 70:4144–4150. <https://doi.org/10.1128/AEM.70.7.4144-4150.2004>.
- Hentschel U, Cary SC, Felbeck H. 1993. Nitrate respiration in chemoautotrophic symbionts of the bivalve *Lucinoma aequizonata*. *Mar Ecol Prog Ser* 94:35–41. <https://doi.org/10.3354/meps094035>.
- Petersen JM, Kemper A, Gruber-Vodicka H, Cardini U, van der Geest M, Kleiner M, Bulgheresi S, Mußmann M, Herbold C, Seah BKB, Antony CP, Liu D, Belitz A, Weber M. 2016. Chemosynthetic symbionts of marine invertebrate animals are capable of nitrogen fixation. *Nat Microbiol* 2:16195. <https://doi.org/10.1038/nmicrobiol.2016.195>.
- Lim SJ, Davis BG, Gill DE, Walton J, Nachman E, Engel AS, Anderson LC, Campbell BJ. 2019. Taxonomic and functional heterogeneity of the gill microbiome in a symbiotic coastal mangrove lucinid species. *ISME J* 13:902–920. <https://doi.org/10.1038/s41396-018-0318-3>.
- König S, Gros O, Heiden SE, Hinzke T, Thurmer A, Poehlein A, Meyer S, Vatin M, Mbeque-A-Mbeque D, Toczny J, Ponnudurai R, Daniel R, Becher D, Schweder T, Markert S. 2016. Nitrogen fixation in a chemoautotrophic lucinid symbiosis. *Nat Microbiol* 2:16193. <https://doi.org/10.1038/nmicrobiol.2016.193>.
- Liljedahl L. 1992. The Silurian *Ilionia prisca*, oldest known deep-burrowing suspension feeding bivalve. *J Paleontol* 66:206–210. <https://doi.org/10.1017/S0022336000033722>.
- Reynolds LK, Berg P, Ziemann JC. 2007. Lucinid clam influence on the biogeochemistry of the seagrass *Thalassia testudinum* sediments. *Estuaries Coast* 30:482–490. <https://doi.org/10.1007/BF02819394>.
- van der Heide T, Govers LL, de Fouw J, Olff H, van der Geest M, van Katwijk MM, Piersma T, van de Koppel J, Silliman BR, Smolders AJP, van Gils JA. 2012. A three-stage symbiosis forms the foundation of seagrass ecosystems. *Science* 336:1432–1434. <https://doi.org/10.1126/science.1219973>.
- Stanley SM. 2014. Evolutionary radiation of shallow-water Lucinidae (Bivalvia with endosymbionts) as a result of the rise of seagrasses and mangroves. *Geology* 42:803–806. <https://doi.org/10.1130/G35942.1>.
- Won Y-J, Hallam SJ, O'Mullan GD, Pan IL, Buck KR, Vrijenhoek RC. 2003. Environmental acquisition of thiotrophic endosymbionts by deep-sea

- mussels of the genus *Bathymodiolus*. Appl Environ Microbiol 69: 6785–6792. <https://doi.org/10.1128/AEM.69.11.6785-6792.2003>.
15. Stewart FJ, Young CR, Cavanaugh CM. 2008. Lateral symbiont acquisition in a maternally transmitted chemosynthetic clam endosymbiosis. Mol Biol Evol 25:673–687. <https://doi.org/10.1093/molbev/msn010>.
 16. Decker C, Olu K, Arnaud-Haond S, Duperron S. 2013. Physical proximity may promote lateral acquisition of bacterial symbionts in vesicomid clams. PLoS One 8:e64830. <https://doi.org/10.1371/journal.pone.0064830>.
 17. Gros O, Darrasse A, Durand P, Frenkiel L, Mouéza M. 1996. Environmental transmission of a sulfur-oxidizing bacterial gill endosymbiont in the tropical lucinid bivalve *Codakia orbicularis*. Appl Environ Microbiol 62: 2324–2330.
 18. Gros O, Wulf-Durand P, Frenkiel L, Mouéza M. 1998. Putative environmental transmission of sulfur-oxidizing bacterial symbionts in tropical lucinid bivalves inhabiting various environments. FEMS Microbiol Lett 160:257–262. [https://doi.org/10.1016/S0378-1097\(98\)00041-X](https://doi.org/10.1016/S0378-1097(98)00041-X).
 19. Gros O, Duplessis MR, Felbeck H. 1999. Embryonic development and endosymbiont transmission mode in the symbiotic clam *Lucinoma aequizonata* (Bivalvia: Lucinidae). Invertebr Reprod Dev 36:93–103. <https://doi.org/10.1080/07924259.1999.9652683>.
 20. Brissac T, Mercot H, Gros O. 2011. Lucinidae/sulfur-oxidizing bacteria: ancestral heritage or opportunistic association? Further insights from the Bohol Sea (the Philippines). FEMS Microbiol Ecol 75:63–76. <https://doi.org/10.1111/j.1574-6941.2010.00989.x>.
 21. Taylor JD, Glover EA. 2016. Lucinid bivalves of Guadeloupe: diversity and systematics in the context of the tropical Western Atlantic (Mollusca: Bivalvia: Lucinidae). Zootaxa 4196:301–380. <https://doi.org/10.11646/zootaxa.4196.3.1>.
 22. Durand P, Gros O. 1996. Bacterial host specificity of Lucinacea endosymbionts: interspecific variation in 16S rRNA sequences. FEMS Microbiol Lett 140:193–198. [https://doi.org/10.1016/0378-1097\(96\)00178-4](https://doi.org/10.1016/0378-1097(96)00178-4).
 23. Durand P, Gros O, Frenkiel L, Prieur D. 1996. Phylogenetic characterization of sulfur-oxidizing bacterial endosymbionts in three tropical Lucinidae by 16S rDNA sequence analysis. Mol Mar Biol Biotechnol 5:37–42.
 24. Gros O, Liberge M, Felbeck H. 2003. Interspecific infection of aposymbiotic juveniles of *Codakia orbicularis* by various tropical lucinid gill-endosymbionts. Mar Biol 142:57–66. <https://doi.org/10.1007/s00227-002-0921-7>.
 25. Brissac T, Higué D, Gros O, Mercot H. 2016. Unexpected structured intraspecific diversity of thioautotrophic bacterial gill endosymbionts within the Lucinidae (Mollusca: Bivalvia). Mar Biol 163:176. <https://doi.org/10.1007/s00227-016-2949-0>.
 26. Edgar RC. 2018. Updating the 97% identity threshold for 16S ribosomal RNA OTUs. Bioinformatics 34:2371. <https://doi.org/10.1093/bioinformatics/bty113>.
 27. Good IJ. 1953. The population frequencies of species and the estimation of population parameters. Biometrika 40:237–264. <https://doi.org/10.2307/2333344>.
 28. Quast C, Pruesse E, Yilmaz P, Gerken J, Schweer T, Yarza P, Peplies J, Glockner FO. 2012. The SILVA ribosomal RNA gene database project: improved data processing and web-based tools. Nucleic Acids Res 41: D590–D596. <https://doi.org/10.1093/nar/gks1219>.
 29. Green-Garcia AM. 2008. Characterization of the lucinid bivalve-bacteria symbiotic system: the significance of the geochemical habitat on bacterial symbiont diversity and phylogeny. Master's thesis. Louisiana State University, Baton Rouge, LA. https://digitalcommons.lsu.edu/gradschool_theses/1970/.
 30. Duperron S, Fiala-Médioni A, Caprais J-C, Olu K, Sibuet M. 2007. Evidence for chemoautotrophic symbiosis in a Mediterranean cold seep clam (Bivalvia: Lucinidae): comparative sequence analysis of bacterial 16S rRNA, APS reductase and RuBisCO genes. FEMS Microbiol Ecol 59:64–70. <https://doi.org/10.1111/j.1574-6941.2006.00194.x>.
 31. Ball AD, Purdy KJ, Glover EA, Taylor JD. 2009. Ctenidial structure and three bacterial symbiont morphotypes in *Anodontia* (*Euanodontia*) ovum (Reeve, 1850) from the Great Barrier Reef, Australia (Bivalvia: Lucinidae). J Molluscan Stud 75:175–185. <https://doi.org/10.1093/mollus/eyp009>.
 32. Espinosa EP, Tanguy A, Le Panse S, Lallier F, Allam B, Boutet I. 2013. Endosymbiotic bacteria in the bivalve *Loripes lacteus*: localization, characterization and aspects of symbiont regulation. J Exp Mar Biol Ecol 448:327–336. <https://doi.org/10.1016/j.jembe.2013.07.015>.
 33. Rodríguez-R LM, Konstantinidis KT. 2014. Bypassing cultivation to identify bacterial species. Microbe 9:111–118. <https://doi.org/10.1128/microbe.9.111.1>.
 34. Brown CT, Olm MR, Thomas BC, Banfield JF. 2016. Measurement of bacterial replication rates in microbial communities. Nat Biotechnol 34:1256–1263. <https://doi.org/10.1038/nbt.3704>.
 35. Aziz RK, Bartels D, Best AA, DeJongh M, Disz T, Edwards RA, Formsma K, Gerdes S, Glass EM, Kubal M, Meyer F, Olsen GJ, Olson R, Osterman AL, Overbeek RA, McNeil LK, Paarmann D, Paczian T, Parrello B, Pusch GD, Reich C, Stevens R, Vassieva O, Vonstein V, Wilke A, Zagnitko O. 2008. The RAST server: rapid annotations using subsystems technology. BMC Genomics 9:75. <https://doi.org/10.1186/1471-2164-9-75>.
 36. Ades SE. 2004. Control of the alternative sigma factor sigmaE in *Escherichia coli*. Curr Opin Microbiol 7:157–162. <https://doi.org/10.1016/j.mib.2004.02.010>.
 37. Nonaka G, Blankschien M, Herman C, Gross CA, Rhodius VA. 2006. Regulation and promoter analysis of the *E. coli* heat-shock factor, sigma32, reveals a multifaceted cellular response to heat stress. Genes Dev 20: 1776–1789. <https://doi.org/10.1101/gad.1428206>.
 38. Lemke JJ, Sanchez-Vazquez P, Burgos HL, Hedberg G, Ross W, Gourse RL. 2011. Direct regulation of *Escherichia coli* ribosomal protein promoters by the transcription factors ppGpp and DksA. Proc Natl Acad Sci U S A 108:5712–5717. <https://doi.org/10.1073/pnas.1019383108>.
 39. Speare L, Cecere AG, Guckes KR, Smith S, Wollenberg MS, Mandel MJ, Miyashiro T, Septer AN. 2018. Bacterial symbionts use a type VI secretion system to eliminate competitors in their natural host. Proc Natl Acad Sci U S A 115:E8528–E8537. <https://doi.org/10.1073/pnas.1808302115>.
 40. Distel DL, Altamia MA, Lin Z, Shipway JR, Han A, Forteza I, Antemano R, Limbaco M, Tebo AG, Dechavez R, Albano J, Rosenberg G, Concepcion GP, Schmidt EW, Haygood MG. 2017. Discovery of chemoautotrophic symbiosis in the giant shipworm *Kuphus polythalamia* (Bivalvia: Teredinidae) extends wooden-steps theory. Proc Natl Acad Sci U S A 114: E3652–E3658. <https://doi.org/10.1073/pnas.1620470114>.
 41. Smejkalova H, Erb TJ, Fuchs G. 2010. Methanol assimilation in *Methylobacterium extorquens* AM1: demonstration of all enzymes and their regulation. PLoS One 5:e13001. <https://doi.org/10.1371/journal.pone.0013001>.
 42. Kobayashi K, Ogata H, Morikawa M, Iijima S, Harada N, Yoshida T, Brown WR, Inoue N, Hamada Y, Ishii H, Watanabe M, Hibi T. 2002. Distribution and partial characterisation of IgG Fc binding protein in various mucin producing cells and body fluids. Gut 51:169–176. <https://doi.org/10.1136/gut.51.2.169>.
 43. Nyholm SV, McFall-Ngai M. 2003. Dominance of *Vibrio fischeri* in secreted mucus outside the light organ of *Euprymna scolopes*: the first site of symbiont specificity. Appl Environ Microbiol 69:3932–3937. <https://doi.org/10.1128/AEM.69.7.3932-3937.2003>.
 44. Liberge M, Gros O, Frenkiel L. 2001. Lysosomes and sulfide-oxidizing bodies in the bacteriocytes of *Lucina pectinata*, a cytochemical and microanalysis approach. Mar Biol 139:401–409. <https://doi.org/10.1007/s002270000526>.
 45. Love MI, Huber W, Anders S. 2014. Moderated estimation of fold change and dispersion for RNA-seq data with DESeq2. Genome Biol 15:550. <https://doi.org/10.1186/s13059-014-0550-8>.
 46. Robinson MD, McCarthy DJ, Smyth GK. 2010. edgeR: a Bioconductor package for differential expression analysis of digital gene expression data. Bioinformatics 26:139–140. <https://doi.org/10.1093/bioinformatics/btp616>.
 47. The UniProt Consortium. 2015. UniProt: a hub for protein information. Nucleic Acids Res 43:D204–D212. <https://doi.org/10.1093/nar/gku989>.
 48. NCBI Resource Coordinators. 2016. Database resources of the National Center for Biotechnology Information. Nucleic Acids Res 44:D7–D19. <https://doi.org/10.1093/nar/gkv1290>.
 49. Mushagian AA, Ebert D. 2016. Rethinking “mutualism” in diverse host-symbiont communities. Bioessays 38:100–108. <https://doi.org/10.1002/bies.201500074>.
 50. Abaibou H, Pommier J, Benoit S, Giordano G, Mandrand-Berthelot M. 1995. Expression and characterization of the *Escherichia coli* *fdo* locus and a possible physiological role for aerobic formate dehydrogenase. J Bacteriol 177:7141–7149. <https://doi.org/10.1128/jb.177.24.7141-7149.1995>.
 51. Croes LM, Meijer WG, Dijkhuizen L. 1991. Regulation of methanol oxidation and carbon dioxide fixation in *Xanthobacter* strain 25a grown in continuous culture. Arch Microbiol 155:159–163. <https://doi.org/10.1007/BF00248611>.
 52. Weis VM, Small AL, McFall-Ngai MJ. 1996. A peroxidase related to the mammalian antimicrobial protein myeloperoxidase in the *Euprymna*

- Vibrio* mutualism. Proc Natl Acad Sci U S A 93:13683–13688. <https://doi.org/10.1073/pnas.93.24.13683>.
53. Small AL, McFall-Ngai MJ. 1999. Halide peroxidase in tissues that interact with bacteria in the host squid *Euprymna scolopes*. J Cell Biochem 72:445–457. [https://doi.org/10.1002/\(SICI\)1097-4644\(19990315\)72:4<445::AID-JCB1>3.0.CO;2-P](https://doi.org/10.1002/(SICI)1097-4644(19990315)72:4<445::AID-JCB1>3.0.CO;2-P).
 54. Davidson SK, Koropatnick TA, Kossmehl R, Sycuro L, McFall-Ngai MJ. 2004. NO means ‘yes’ in the squid-vibrio symbiosis: nitric oxide (NO) during the initial stages of a beneficial association. Cell Microbiol 6:1139–1151. <https://doi.org/10.1111/j.1462-5822.2004.00429.x>.
 55. Cascales E, Buchanan SK, Duche D, Kleanthous C, Lloubes R, Postle K, Riley M, Slatin S, Cavard D. 2013. Colicin biology. Microbiol Mol Biol Rev 71:158–229. <https://doi.org/10.1128/MMBR.00036-06>.
 56. Green ER, Meccas J. 2016. Bacterial secretion systems: an overview, p 215–239. In Kudva I, Cornick N, Plummer P, Zhang Q, Nicholson T, Bannantine J, Bellaire B (ed), Virulence mechanisms of bacterial pathogens, 5th ed. ASM Press, Washington, DC.
 57. Nivaskumar M, Francetic O. 2014. Type II secretion system: a magic beanstalk or a protein escalator. Biochim Biophys Acta 1843:1568–1577. <https://doi.org/10.1016/j.bbamcr.2013.12.020>.
 58. Garcia-Horsman JA, Barquera B, Rumbley J, Ma J, Gennis RB. 1994. The superfamily of heme-copper respiratory oxidases. J Bacteriol 176:5587–5600. <https://doi.org/10.1128/jb.176.18.5587-5600.1994>.
 59. Pitcher RS, Watmough NJ. 2004. The bacterial cytochrome cbb3 oxidases. Biochim Biophys Acta 1655:388–399. <https://doi.org/10.1016/j.bbabi.2003.09.017>.
 60. Borisov VB, Gennis RB, Hemp J, Verkhovsky MI. 2011. The cytochrome bd respiratory oxygen reductases. Biochim Biophys Acta 1807:1398–1413. <https://doi.org/10.1016/j.bbabi.2011.06.016>.
 61. Kaminski PA, Kitts CL, Zimmerman Z, Ludwig RA. 1996. *Azorhizobium caulinodans* uses both cytochrome bd (quinol) and cytochrome cbb3 (cytochrome c) terminal oxidases for symbiotic N₂ fixation. J Bacteriol 178:5989–5994. <https://doi.org/10.1128/jb.178.20.5989-5994.1996>.
 62. Poole RK, Hill S. 1997. Respiratory protection of nitrogenase activity in *Azotobacter vinelandii*—roles of the terminal oxidases. Biosci Rep 17:303–317. <https://doi.org/10.1023/A:1027336712748>.
 63. Dincturk HB, Demir V, Aykanat T. 2011. Bd oxidase homologue of photosynthetic purple sulfur bacterium *Allochrochromatium vinosum* is co-transcribed with a nitrogen fixation related gene. Antonie Van Leeuwenhoek 99:211–220. <https://doi.org/10.1007/s10482-010-9478-5>.
 64. Bianucci E, Furlan A, Castro S. 2017. Importance of glutathione in the legume-Rhizobia symbiosis, p 373–396. In Hossain MA, Mostofa MG, Diaz-Vivancos P, Burritt DJ, Fujita M, Tran LP (ed), Glutathione in plant growth, development, and stress tolerance. Springer International Publishing, Cham, Switzerland.
 65. Tabita FR, Satagopan S, Hanson TE, Kreel NE, Scott SS. 2007. Distinct form I, II, III, and IV RuBisCO proteins from the three kingdoms of life provide clues about RuBisCO evolution and structure/function relationships. J Exp Bot 59:1515–1524. <https://doi.org/10.1093/jxb/erm361>.
 66. Kraus DW, Wittenberg JB. 1990. Hemoglobins of the *Lucina pectinata*/bacteria symbiosis. I. Molecular properties, kinetics and equilibria of reactions with ligands. J Biol Chem 27:16043–16053.
 67. Dibrova DV, Cherepanov DA, Galperin MY, Skulachev VP, Mulkidjanian AY. 2013. Evolution of cytochrome bc complexes: from membrane-anchored dehydrogenases of ancient bacteria to triggers of apoptosis in vertebrates. Biochim Biophys Acta 1827:1407–1427. <https://doi.org/10.1016/j.bbabi.2013.07.006>.
 68. Van Vranken JG, Na U, Winge DR, Rutter J. 2015. Protein-mediated assembly of succinate dehydrogenase and its cofactors. Crit Rev Biochem Mol Biol 50:168–180. <https://doi.org/10.3109/10409238.2014.990556>.
 69. Marcia M, Ermler U, Peng G, Michel H. 2010. A new structure-based classification of sulfide:quinone oxidoreductases. Proteins 78:1073–1083. <https://doi.org/10.1002/prot.22665>.
 70. Nishiguchi MK. 2000. Temperature affects species distribution in symbiotic populations of *Vibrio* spp. Appl Environ Microbiol 66:3550–3555. <https://doi.org/10.1128/AEM.66.8.3550-3555.2000>.
 71. Gros O, Elisabeth NH, Gustave SD, Caro A, Dubilier N. 2012. Plasticity of symbiont acquisition throughout the life cycle of the shallow-water tropical lucinid *Codakia orbiculata* (Mollusca: Bivalvia). Environ Microbiol 14:1584–1595. <https://doi.org/10.1111/j.1462-2920.2012.02748.x>.
 72. Elisabeth NH, Gustave SDD, Gros O. 2012. Cell proliferation and apoptosis in gill filaments of the lucinid *Codakia orbiculata* (Montagu, 1808) (Mollusca: Bivalvia) during bacterial decolonization and recolonization. Microsc Res Tech 75:1136–1146. <https://doi.org/10.1002/jemt.22041>.
 73. Elisabeth NH, Caro A, Cesaire T, Mansot J, Escalas A, Sylvestre M, Jean-Louis P, Gros O. 2014. Comparative modifications in bacterial gill-endosymbiotic populations of the two bivalves *Codakia orbiculata* and *Lucina pensylvanica* during bacterial loss and reacquisition. FEMS Microbiol Ecol 89:646–658. <https://doi.org/10.1111/1574-6941.12366>.
 74. Brissac T, Gros O, Mercot H. 2009. Lack of endosymbiont release by two Lucinidae (Bivalvia) of the genus *Codakia*: consequences for symbiotic relationships. FEMS Microbiol Ecol 67:261–267. <https://doi.org/10.1111/j.1574-6941.2008.00626.x>.
 75. Burke C, Steinberg P, Rusch D, Kjelleberg S, Thomas T. 2011. Bacterial community assembly based on functional genes rather than species. Proc Natl Acad Sci U S A 108:14288–14293. <https://doi.org/10.1073/pnas.11015911108>.
 76. Schloss PD, Westcott SL, Ryabin T, Hall JR, Hartmann M, Hollister EB, Lesniewski RA, Oakley BB, Parks DH, Robinson CJ, Sahl JW, Stres B, Thallinger GG, Van Horn DJ, Weber CF. 2009. Introducing mothur: open-source, platform-independent, community-supported software for describing and comparing microbial communities. Appl Environ Microbiol 75:7537–7541. <https://doi.org/10.1128/AEM.01541-09>.
 77. Langmead B, Salzberg SL. 2012. Fast gapped-read alignment with Bowtie 2. Nat Methods 9:357–359. <https://doi.org/10.1038/nmeth.1923>.
 78. Li H, Handsaker B, Wysoker A, Fennell T, Ruan J, Homer N, Marth G, Abecasis G, Durbin R, 1000 Genome Project Data Processing Subgroup. 2009. The sequence alignment/map format and SAMtools. Bioinformatics 25:2078–2079. <https://doi.org/10.1093/bioinformatics/btp352>.
 79. Haas BJ, Papanicolaou A, Yassour M, Grabherr M, Blood PD, Bowden J, Couger MB, Eccles D, Li B, Lieber M, MacManes MD, Ott M, Orvis J, Pochet N, Strozzi F, Weeks N, Westerman R, William T, Dewey CN, Henschel R, LeDuc RD, Friedman N, Regev A. 2013. *De novo* transcript sequence reconstruction from RNA-Seq: reference generation and analysis with Trinity. Nat Protoc 8:1494–1512. <https://doi.org/10.1038/nprot.2013.084>.
 80. Liao Y, Smyth GK, Shi W. 2014. featureCounts: an efficient general purpose program for assigning sequence reads to genomic features. Bioinformatics 30:923–930. <https://doi.org/10.1093/bioinformatics/btt656>.
 81. Suomi T, Seyednasrollah F, Jaakkola MK, Faux T, Elo LL. 2017. ROTS: an R package for reproducibility-optimized statistical testing. PLoS Comput Biol 13:e1005562. <https://doi.org/10.1371/journal.pcbi.1005562>.
 82. Law CW, Chen Y, Shi W, Smyth GK. 2014. voom: precision weights unlock linear model analysis tools for RNA-seq read counts. Genome Biol 15:R29. <https://doi.org/10.1186/gb-2014-15-2-r29>.
 83. Young MD, Wakefield MJ, Smyth GK, Oshlack A. 2010. Gene ontology analysis for RNA-seq: accounting for selection bias. Genome Biol 11:R14. <https://doi.org/10.1186/gb-2010-11-2-r14>.
 84. Ritchie ME, Phipson B, Wu D, Hu Y, Law CW, Shi W, Smyth GK. 2015. *limma* powers differential expression analyses for RNA-seq and microarray studies. Nucleic Acids Res 43:e47. <https://doi.org/10.1093/nar/gkv007>.
 85. The Gene Ontology Consortium. 2015. Gene ontology consortium: going forward. Nucleic Acids Res 43:D1049–D1056. <https://doi.org/10.1093/nar/gku1179>.
 86. Benjamini Y, Hochberg Y. 1995. Controlling the false discovery rate: a practical and powerful approach to multiple testing. J R Stat Soc B 57:289–300. <https://doi.org/10.1111/j.2517-6161.1995.tb02031.x>.
 87. Oliveros JC. 2007. Venny, an interactive tool for comparing lists with Venn’s diagrams. BioinfoGP Service, Centro Nacional de Biotecnología (CNB-CSIC), Madrid, Spain.
 88. Benson DA, Clark K, Karsch-Mizrachi I, Lipman DJ, Ostell J, Sayers EW. 2014. GenBank. Nucleic Acids Res 42:D32–D37. <https://doi.org/10.1093/nar/gkt1030>.
 89. Anisimova M, Gascuel O. 2006. Approximate likelihood-ratio test for branches: a fast, accurate, and powerful alternative. Syst Biol 55:539–552. <https://doi.org/10.1080/10635150600755453>.
 90. Vorholt JA. 2002. Cofactor-dependent pathways of formaldehyde oxidation in methylotrophic bacteria. Arch Microbiol 178:239–249. <https://doi.org/10.1007/s00203-002-0450-2>.
 91. Pomper BK, Saurel O, Milon A, Vorholt JA. 2002. Generation of formate by the formyltransferase/hydrolase complex (Fhc) from *Methylobacterium extorquens* AM1. FEBS Lett 523:133–137. [https://doi.org/10.1016/S0014-5793\(02\)02962-9](https://doi.org/10.1016/S0014-5793(02)02962-9).
 92. Shorthouse DP. 2010. SimpleMapp, an online tool to produce publication-quality point maps. <https://www.simplemapp.net>.